



TAMPEREEN TEKNILLINEN YLIOPISTO
TAMPERE UNIVERSITY OF TECHNOLOGY

SELIMCAN DEDA
SMART BATTERY POWER MANAGEMENT UNIT
Master of Science Thesis

Examiners: Prof. Nikolay T. Tchamov
MSc. Jani Järvenhaara

Examiners and topic approved by the
Faculty Council of the Faculty of
Electrical Engineering on 3 April 2013.

ABSTRACT

TAMPERE UNIVERSITY OF TECHNOLOGY

Master's Degree Programme in Electrical Engineering

DEDA, SELIMCAN: Smart Battery Power Management Unit

Master of Science Thesis, 73 pages, 6 Appendix pages

February 2014

Major: Radio Frequency Electronics

Examiners: Professor Nikolay T. Tchamov and MSc. Jani Järvenhaara

In this project, the ways how a Smart 48V Battery Power Management Unit (PMU) which uses lead-acid batteries can be designed for wide range of industry usage are researched.

PMU is a modified version of Battery Management System (BMS). Since the batteries are designed for charging and discharging for their life, they need an optimum way to be monitored and/or balanced to increase their efficiency. The PMU system monitors the voltages and State-of-Charges (SoCs) of whole battery module & individual cells. PMU ensures reliable and safe battery operations.

MAX11068 is used in the project to meet the monitoring and/or balancing requirements of the BMS, and thus PMU. However, only using the MAX11068 is not enough for designing a PMU. In addition to the MAX11068, a microcontroller (Arduino Due) and a comprehensive Java program are used in the PMU project. The microcontroller is programmed so that it sends to and receives information from the Java program. The GUI application is included to let users to investigate the voltage and SoC variations in whole battery module & individual cells. The users also have an option to write the data to Microsoft Office Excel sheet. Therefore, they can make use of it whenever they want.

The complete PMU system monitors the voltages and SoCs of whole battery module and individual cells accurately. Moreover, the GUI displays the changes the voltages and SoCs of whole battery module and individual cells on the SoC and voltage charts.

At the end of the project, the theoretical knowledge is compared with experimental results.

PREFACE

First and foremost, I would like to thank my supervisor, Professor Nikolay T.Tchamov, who gave me the opportunity to join the RF Integrated Circuits Laboratory and for his guidance, advice, encouragement and unwavering enthusiasm throughout my working time as research assistantship. At many stages of this research project I have utilized from his experiences to explore new ideas.

I would thank to my examiner Jani Järvenhaara for spending his time to revise my MSc. Thesis and for his precious comments to make my MSc. Thesis well.

I also would like to thank my dear past and present group members in RF Integrated Circuits Laboratory for their friendship, help and suggestions to accomplish my MSc. Thesis project. It is due them that I have enjoyed my working time in RF Integrated Circuits Laboratory.

Next I would like to address my friends from Finland. I have met so many nice people from different cultures during my stay in Finland. You made my time so special and memorable in Finland.

Additional thanks go to my special friends from Turkey and all around world for providing support and valuable friendship that I need throughout my life.

To Meriç Çağlar, my oldest friend, you are truly more than a special friend, a brother I call you. Thank you for always giving me motivation to work harder.

I am indebted to my mother for teaching me to hold my head high in life, my father for giving me advices when I am undecided about anything in life and my family for their priceless help and support. I am truly gifted to have you as part of my life.

Lastly, I want to dedicate my MSc. Thesis to soul of my dear grandmother who untimely passed away during the last stage of my MSc. Thesis work and my dear uncle who passed away long time ago. I believe if they were still alive, they would be proud of me.

Selimcan Deda

Tampere, February 2014

CONTENTS

List of Figures	v
List of Tables	vii
List of Abbreviations	viii
List of Symbols	x
1. Introduction.....	1
2. Literature Review.....	2
2.1. What does Battery Management System (BMS) mean?	2
2.1.1. The Functions of Power Management Unit (PMU).....	2
2.1.2. Application Areas of PMU	3
2.2. Cell Balancing Methods for PMU.....	5
2.3. Lead-Acid Batteries.....	6
2.3.1. The History and Present of Lead-Acid Batteries	6
2.3.2. Charging Lead-Acid Batteries	7
2.3.2.1 Constant Current/Constant Voltage Charging.....	7
2.3.3. Comparison of Rechargeable Batteries.....	9
2.3.4. Future of Lead-Acid Batteries	11
2.4. State of Charge (SoC) Calculations	11
2.4.1. The SoC Calculation Methods	11
2.5. State of Health (SoH) Estimations	13
3. System Considerations Based on MAX11068.....	16
3.1. Inter-Integrated Circuit (I ² C) Communication.....	16
3.1.1. Serial Data Line (SDA) and Serial Clock Line (SCL).....	17
3.1.2. I ² C Command List	19
3.2. MAX11068.....	22
3.2.1. Analog-to-Digital Converter (ADC).....	24
3.3. Jumper/Switch Configurations and Cell Connections	24
3.4. Starting up the MAX11068 EV kit	25
3.4.1. MAX11068 EVKit SMBus Ladder	27
3.5. Arduino Due	28
3.6. Comparison of Selected BMS Boards.....	30
4. Power Management System Design	32
5. Programming of Power Management Unit.....	36
5.1. Flowchart of Programming of PMU	36

5.2. Java Libraries	38
5.3. State of Charge (SoC) Calculation Function.....	38
6. Results and Discussion	39
6.1. Graphical User Interface	39
6.2. Cell Measurement Results.....	40
6.2.1. GUI Chart Results.....	42
6.2.2. Excel Results.....	44
6.3. Load Discharging Curve	45
7. Conclusions.....	49
8. Continuation Design of Work.....	50
References.....	52
Appendix 1: MAX11068 EVKit Cell Configuration Headers and Switch.....	57
Appendix 2: MAX11068 EVKit Cell Connection Switches and Headers	60
Appendix 3: Discharging Energys Cyclon Batteries.....	61
Appendix 4: Timing of Parameter Updates During the Relaxation Mode for State of Health Estimation.....	62

LIST OF FIGURES

Figure 1. General PMU Block Diagram	3
Figure 2. Some examples of application areas of PMU.....	3
Figure 3. Power (in MW) vs. time (Wikipedia 2009).....	4
Figure 4. Cost vs. Increasing Renewable Energy Penetration (Begovic 2012).....	5
Figure 5. Charge Current vs. Charging Time for three different current limits (Linden et al. 2002)	8
Figure 6. Hyperion AC/DC EOS0606iAD-C battery charger (Hyperion 2013)	9
Figure 7. Enersys Cyclon Battery Open Circuit Voltage vs. State of Charge (Enersys Cyclon 2008).....	12
Figure 8. I ² C-bus bit transmission (NXP Semiconductors 2012).....	17
Figure 9. START and STOP conditions (NXP Semiconductors 2012).....	17
Figure 10. Complete Data Transfer (NXP Semiconductors 2012).....	18
Figure 11. Functional Communication Initialization Sequence Diagram of MAX11068 (Maxim Integrated 2010)	21
Figure 12. Functional Block Diagram of MAX11068 (Maxim Integrated 2010)	22
Figure 13. MAX11068 EVKit (Maxim Integrated).....	23
Figure 14. MAX11068 EVKit SMBus Ladder when Board (A) is first board (Maxim Integrated MAX11068 Evaluation System 2010).....	27
Figure 15. The front view of Arduino Due (Arduino).....	28
Figure 16. The complete measurement system.....	32
Figure 17. Connection Setup of MAX11068.....	32
Figure 18. Series connected Lead-Acid battery design	33
Figure 19. Arduino Due & J3 Header of MAX11068 Evaluation Kit+ PACK A Connection	33
Figure 20. Load design	34
Figure 21. Complete system setup.....	35
Figure 22. The flowchart of programming of PMU	37
Figure 23. PMU GUI without charts.....	39
Figure 24. Individual cell voltages and SoCs	40
Figure 25. Total Battery SoC vs. Time.....	42
Figure 26. Total Battery SoC vs. Time in a different period of time.....	42
Figure 27. Total Battery Voltage vs. Time	43

Figure 28. Total Battery Voltage vs. Time in a different period of time	43
Figure 29. Instantaneous Battery Voltage, SoC and Status	44
Figure 30. Cell voltages and measurement counter displayed in Excel sheet	44
Figure 31. Cell SoC and date & time displayed in Excel sheet	45
Figure 32. Total lead-acid battery voltage versus time.....	46
Figure 33. Load Discharging Curve of lead-acid battery cell #19.....	46
Figure 34. Future BMS/PMU Block Diagram.....	50

LIST OF TABLES

Table 1. Specifications of Hyperion AC/DC EOS0606iAD-C (Hyperion).....	8
Table 2. Characteristics of different rechargeable batteries (Pistoia 2005).....	9
Table 3. Advantages and disadvantages of lead-acid batteries compared to other rechargeable battery types (Linden et al. 2002).....	10
Table 4. Characteristics of Lead-Acid Batteries (Broussely et al. 2007 & Pistoia 2009). 10	
Table 5. Open Circuit Voltage vs. State of Charge of lead-acid battery cell.....	13
Table 6. Definition of I ² C-bus terminology.....	16
Table 7. I ² C Command List (Maxim Integrated 2010).....	19
Table 8. I ² C-bus Address Bits (Maxim Integrated 2010).....	20
Table 9. Jumper Configurations based on number of cells of MAX11068 EVALUATION KIT+ PACK A & B.....	24
Table 10. Header P3 Cell Connections of MAX11068 EVALUATION KIT+ PACKA. 25	
Table 11. Jumper Configurations of MAX11068 EVALUATION KIT+ PACK A & B. 25	
Table 12. Switch Configurations of MAX11068 EVALUATION KIT+ PACK A & B . 26	
Table 13. J3 Header Pinout of MAX11068 EVALUATION KIT+ PACK A.....	26
Table 14. J1 Header Pinout of MAX11068 EVALUATION KIT+ PACK A.....	27
Table 15. J2 Header Pinout of MAX11068 EVALUATION KIT+ PACK A.....	28
Table 16. Pin mapping of Arduino Due that used in system.....	29
Table 17. Comparison of Different BMS Evaluation Kits.....	30
Table 18. The used core Java libraries.....	38
Table 19. SoC (%) and SoC Icon with respect to it.....	41
Table 20. Comparison of GUI and multimeter lead-acid battery cell measurements.....	48

LIST OF ABBREVIATIONS

ACK	acknowledge
ADC	analog-to-digital converter
BMS	battery management system
CC	constant current
CC/CV	constant current/constant voltage
COM	communication
CV	constant voltage
DC	direct current
DoD	depth of discharge
EODV	end of discharge voltage
EV	electric vehicle
EVKit	evaluation kit
FCC	full charge capacity
FET	field-effect transistor
FWUP	faster wakeup
GND	ground
GPS	global positioning system
GUI	graphical user interface
IC	integrated circuit
I ² C	inter-integrated circuit
I/O	input/output
JU	jumper
KERS	kinetic energy recovery system
LDO	low-dropout regulator
LED	light-emitting diode
LSB	least significant bit
Max	maximum
Min	minimum
MOS	metal-oxide-semiconductor
MOSFET	metal-oxide-semiconductor field-effect transistor
MSB	most significant bit
NACK	negative-acknowledge

NTC	negative temperature coefficient
N/A	not available
OCV	open circuit voltage
OV	overcharge
PC	personal computer
PEC	packet-error checking
PMU	power management unit
PWM	pulse width modulation
RF	radio frequency
RTD	resistance temperature detector
RX	receiver
R/W	read/write
SCL	serial clock line
SDA	serial data line
SMBus	system management bus
SoC	state of charge
SoH	state of health
SLI	starting lighting ignition
SR	repeated start
SW	switch
TV	television
TX	transmitter
UPS	uninterruptible power system
USB	universal serial bus
UV	undercharge
V_{DD}	positive supply voltage of FET
VDDBU	backup voltage
V_{IH}	high-level input voltage
V_{IL}	low-level input voltage
XOR	exclusive OR

LIST OF SYMBOLS

$ADC(out)$	output of analog-to-digital conversion
$C(x)$	CRC-8 polynomial
DoD	depth of discharge
FCC	full charge capacity
I_D	drain current
P_D	power dissipation
Q_{max}	maximum battery capacity
Q_{passed}	passed charge
Q_{start}	charge at the beginning
R_G	gate resistor
RM	remained capacity
R_S	sensing resistor
SoC	state of charge
SoH	state of health
V_{bat}	battery voltage
V_{BE}	base-emitter voltage

1. INTRODUCTION

The devices that obtain some or all of their running power from a battery have become widespread in various industries. The fast enlargement of the use of EVs, portable electronic devices, remotely operated devices and renewable energy systems generates high demand for fast propagation of battery technologies (Bergveld et al. 2002).

This project is done because there are only limited applications of smart BMS or PMU which work with commercially available lead-acid batteries. The main goal of this MSc. project is to design an accurate and safe PMU monitoring for a certain cell stack size; including voltage and SoC measurements of battery module and individual cells for different charging conditions.

In 2011, various German automobile manufacturers proposed using 48V electrical system standard to obtain higher power than systems using 12V electrical system standard (Miller 2012). This MSc. Thesis which deals with 48V lead-acid batteries is part of a larger KERS project (Tampere University of Technology RF Integrated Circuits Laboratory 2013) that is going to provide energy interaction with DC/DC converter and motor controller for mobile & stationary big volume applications.

In this MSc. Thesis, the ways how a smart battery PMU can be designed for wide range of applications are researched. The theoretical background is going to be given before explaining the PMU research methods and materials. The PMU, a modified version of BMS, is going to be discussed. The boards which can be used for designing PMU are going to be compared and the reason of selection of the MAX11068 EVKit is going to be explained. Moreover, the lead-acid batteries are going to be discussed further. The importance of SoC and SoH estimations are going to be explained. Thereafter, the setup process of PMU is going to be stated. The flowchart of smart battery PMU programming is going to be illustrated. Next, the results of PMU are going to be given and discussed. After that, the conclusion of PMU project is going to be drawn. Lastly, the continuation design of work is going to be stated.

2. LITERATURE REVIEW

2.1. What does Battery Management System (BMS) mean?

According to Andrea (2010), BMS means that; to monitor all cell voltages, protect the battery cells, estimate the battery's state of charge, extend battery life, maximize the battery's performance, and control the load.

2.1.1. The Functions of Power Management Unit (PMU)

The PMU, a modified version of a BMS, has crucial power functions in addition to its battery management functions (Andrea 2010). This is the main difference of BMS and PMU.

The main function of BMS is to protect all battery cells via keeping them within a safe operating range. Furthermore, the top balancing (approximately 100% State of Charge (SoC)) is preferred. In brief, the BMS is an intelligent charging/discharging system.

Additionally, the battery operated devices and systems have to be managed to work in their optimum levels. The battery operated devices can be consisted of a large number of battery cells, and so high voltage levels. For this purpose, the PMU can be designed to provide optimum use of battery powered devices by maximizing battery capacity and life, reducing the risks of damaging those devices and controlling the charging voltage safely. This can be accomplished by controlling (i.e. cell balancing) and/or monitoring the charging and discharging processes of battery powered devices.

The monitor of PMU can measure and show the figures of merit of conditions of a battery which are voltage, SoC, State of Health (SoH) and temperature during charging and discharging based on the requirement of users. However, the monitor of PMU cannot directly impede the current. In addition to those similar BMS functions, PMU can alter the effective power-supply source from batteries (Wang et al. 2010). PMU can provide low power consumption in system without affecting the system functions which separates it from BMS.

Consequently, PMUs are connectors between batteries and battery operated devices/systems which enhance battery performance and device/system operation in a reliable and safe way.

In Figure 1, an example of usage of PMU is given.

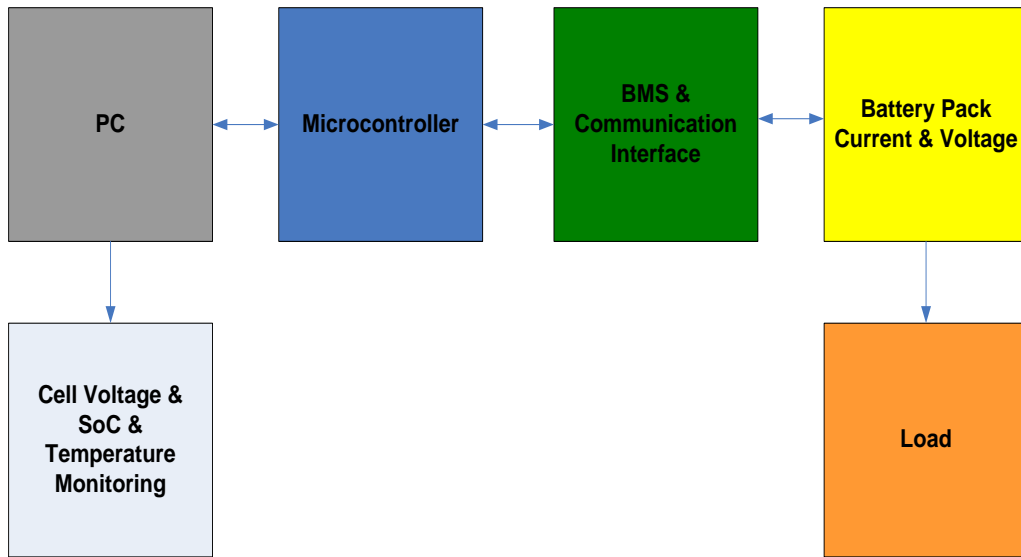


Figure 1. General PMU Block Diagram

In Figure 1, the load can be consisted of motor, DC/DC converters, switches, rectifiers, power metal-oxide-semiconductor field-effect transistors (MOSFETs) and pumps.

2.1.2. Application Areas of PMU

PMU has a wide range of applications; from military to medical:

- ✓ Automotive Industry (i.e. Electric and Hybrid Vehicles),
- ✓ Renewable Energy Systems (i.e. Solar, Wind, Green, and Smart-Sustainable Grid Renewable Energy Systems),
- ✓ Military (i.e. Military Radios),
- ✓ Navigators (i.e. global positioning system (GPS)), and
- ✓ Portable Medical Systems (i.e. Heart Monitors and Defibrillators).

In Figure 2, four application areas of PMU are shown (forklifts, golf carts, shavers, and electric vehicles; respectively).



Figure 2. Some examples of application areas of PMU

Nonetheless, since a smart battery PMU prolongs the battery life, it can be used to reduce the cost of vehicle during its entire lifetime. Therefore, electric vehicle (EV) batteries get vehicle manufacturer's attention. According to Claus, EVs can decrease the gasoline consumption up to 75% (2008). Moreover, according to the Boston Consulting Group Inc. (2010), in 2020 the Electric Vehicle batteries market is expected to reach US\$25 billion in Western Europe, Japan, United States and China. High quality, reliable, safe, monitorable and controllable batteries are needed to meet those expectations and to optimize life of the EVs. Hence, EV manufacturers should consider not only batteries but also PMUs in rapidly growing EV markets.

Furthermore, the energy storage curves of load power, generated power (with and without energy storage) and energy flow to storage for the experiment of one day are given in Figure 3.

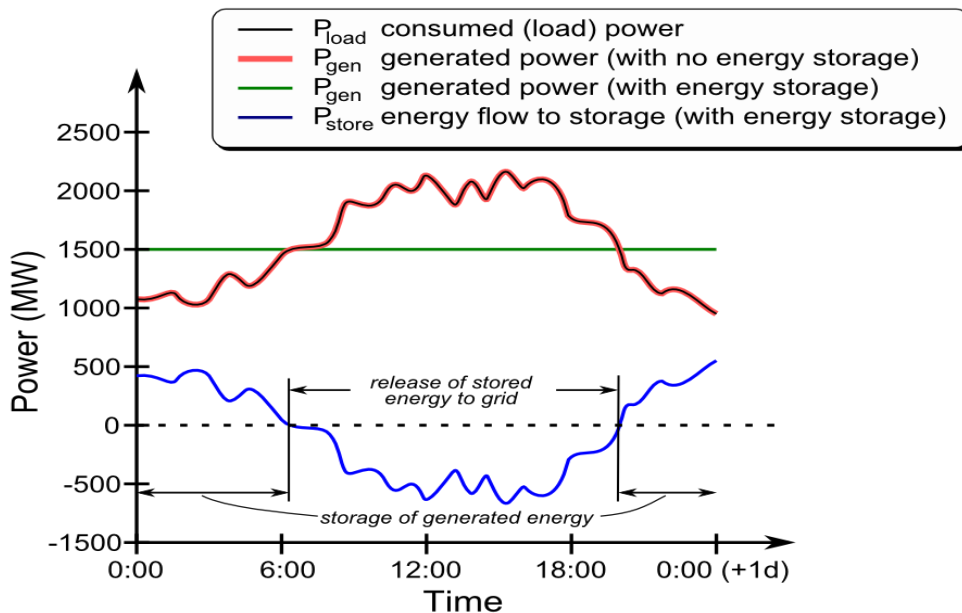


Figure 3. Power (in MW) vs. time (Wikipedia 2009)

It is obtained from the Figure 3 that the electrical energy which is produced by natural resources is varied during the day according to different conditions. It directly affects the energy storage. However, the energy resources should be adjusted well if there is no energy storage. For this purpose, PMU can be used for distributed energy storage. The main challenges of battery energy storage are controlling battery lifetime, power delivery, providing safety, and handling costs (Rahimi-Eichi et al. 2013). Those challenges can be completed via PMU.

According to National Geographic (2004), the oil supplies of world are going to be depleted in 2057. Therefore, battery-powered EVs are going to be needed in future for

providing required energy. The PMU is going to play a crucial role in controlling and optimizing energy storage devices and systems in EVs accurately.

Figure 4 shows the flexibility supply curve.

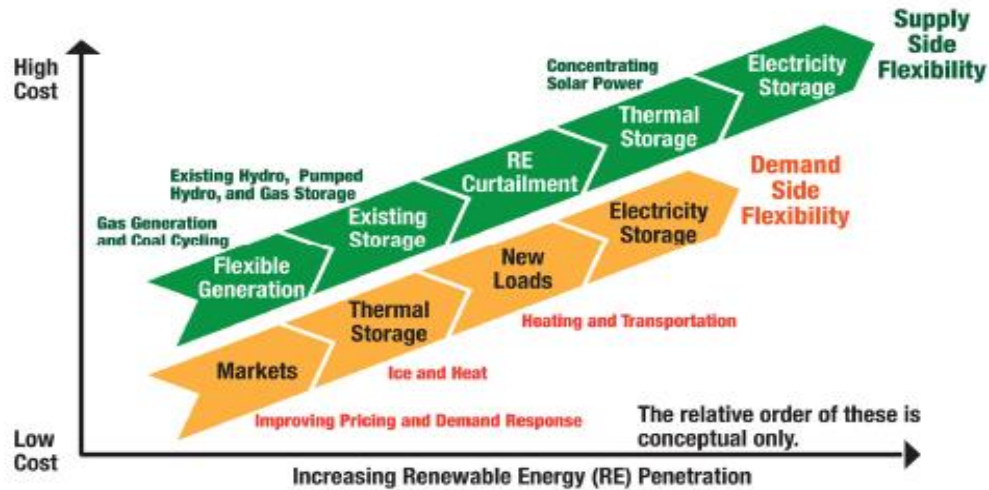


Figure 4. Cost vs. Increasing Renewable Energy Penetration (Begovic 2012)

Figure 4 describes the various approaches of ensuring system flexibility which is required for defragmenting renewable energy sources. It also shows the variation in conceptual cost demand of several systems which ensure the integration in electrical system including supplemental flexibility. The PMU technology may help to manage the system and decrease risks within this chain.

The improvement of 48V EV motors via PMU with battery fuel gauges provides some opportunities in electric vehicles industry. The PMU is able to monitor the battery status and it may control the battery recharging via energy recovery (Pistoia 2005). In 2011, some German automobile manufacturing companies proposed using 48V electrical system standard to acquire more power than the systems using 12V electrical system standard while considering 60V electric shock limit of EVs for safety issues (Miller 2012). Therefore, EVs need a leading-edge technology such as PMU.

2.2. Cell Balancing Methods for PMU

The PMU may protect the battery by stopping the charging current if any cell voltage exceeds the limit. Moreover, if the temperature also exceeds the limit, then the PMU can stop the charging current to protect the battery. Similarly, if any cell voltage drops below the limit, then the PMU may stop the discharging current. For those operations the PMU uses a well-known function called cell balancing. Cell balancing can be either active or passive (Andrea 2010).

When the lead-acid battery cells are connected in series, the current has a direct effect on all of the cells. If the cell voltages start to differentiate, the charges become unbalanced which may cause a battery malfunctioning for very long cell series strings at the end. Hence, a battery balancing mechanism can be used to prevent this potential failure (Krein et al. 2002).

The capacity of a lead-acid battery can be maximized with cell balancing by extending two limiting (lowest & highest) points (Arendarik 2012). Those two limits are defined by one cell in a balanced battery. The charge is removed via preventing the charging current from the most charged cell and an extra charging current is provided to weakest charged cell.

In passive balancing the energy is squandered as heat and in active balancing the energy is transmitted between cells. The passive balancing method of array of cells in series can be used for lead-acid batteries (Krein et al. 2002). On the contrary, the active balancing method is not depending on chemical properties of the battery cells. There are both advantages and disadvantages of passive and active balancing. The passive balancing method wastes power, but its implementation is easier than the active balancing method. On the other hand, the active balancing method is faster and the power efficiency of active balancing method is higher than the passive balancing method, but the active balancing method is more complex and expensive than the passive balancing method (Krein et al. 2002).

The cell balancing is optional for series connected 24 battery cells in this smart battery PMU project. However, hundreds of battery cells totaling hundreds of volts are required to power electric motors (Miller 2012). If hundreds of series connected battery cells are used for applications then the cell balancing should be implemented to increase the efficiency of battery-powered devices and systems.

2.3. Lead-Acid Batteries

2.3.1. The History and Present of Lead-Acid Batteries

The first practical lead-acid battery was invented by Gaston Planté in 1860 (Linden et al. 2002) and it was the first rechargeable battery for industrial and commercial use. Planté's lead-acid battery cells had a low charging capacity. Following Planté's inventions, lead-acid batteries were developed further and they are being developed now. The lead-acid batteries are still popular and manufactured globally although they are older than other rechargeable batteries. Typically, lead-acid batteries are nowadays used in automotive, electric vehicle, submarine, uninterruptible power system (UPS), television (TV), radio and alarm systems industries.

2.3.2. Charging Lead-Acid Batteries

The recharging process is crucial for batteries to secure the optimum life for them. At below, three main steps for recharging Lead-Acid batteries are given (Reddy 2011).

1. At the beginning of recharging process, the charging current should not generate an average battery cell voltage which is greater than 2.4V (gassing threshold). For cyclic applications, the charging current should not generate an average battery cell voltage which is greater than 2.5V (Energys Cyclon 2008).
2. The charging current should be managed so that the cell voltage is kept lower than 2.4V (for cyclic applications, cell voltage is kept lower than 2.5V) during the recharging process and till 100% of previous discharging capacity is achieved.
3. The current starts to decay to charge finishing rate when the battery begins to saturate. The recharging process should be ended up at a constant current which is not more than that charge finishing rate.

There are three main methods for recharging batteries: Constant Current (CC) charging method, Constant Voltage (CV) charging method or Constant Current/Constant Voltage (CC/CV) charging method can be used depending on certain conditions.

First of all, since current adjustment is required if the charging current is not restrained at a low level, the recharging duration becomes longer. Therefore, the CC charging method is not broadly used for recharging lead-acid batteries. On the other hand, for charging Energys Cyclon Lead-Acid batteries the CC/CV charging can be used because it applies single constant current/voltage level across the battery terminals regardless of lead-acid batteries' SoC which are suitable for recharging lead-acid batteries. Moreover, CC/CV chargers ensure high preliminary current to the lead-acid batteries due to the high voltage difference between the charger and lead-acid batteries.

According to Energys Cyclon (2008), constant voltage charging method is suggested for charging lead-acid batteries when no current limit is required. Therefore, CC/CV charging method should be applied when a current limit is required.

2.3.2.1 Constant Current/Constant Voltage Charging

According to Linden et al. (2002), modified constant potential with initial constant current charging method is the fastest and most effective way to recharge lead-acid batteries. In CC/CV method, a constant voltage with initial constant current is applied to battery to recharge it. The charging current is at its peak at the beginning of charging process. Moreover, it is strongly suggested by Energys Cyclon (2008) that the charging voltage has to be kept in the range of 2.45V to 2.5V per cell for cyclic applications. If the

charging voltage is less than 2.45V per cell then there might happen a quick loss in cell capacity.

In Figure 5, changes in charge current in time are given for 2.5Ah battery charged by constant voltage of 2.45V. Moreover, chargers are limited to 0.3A, 1A and 2A.

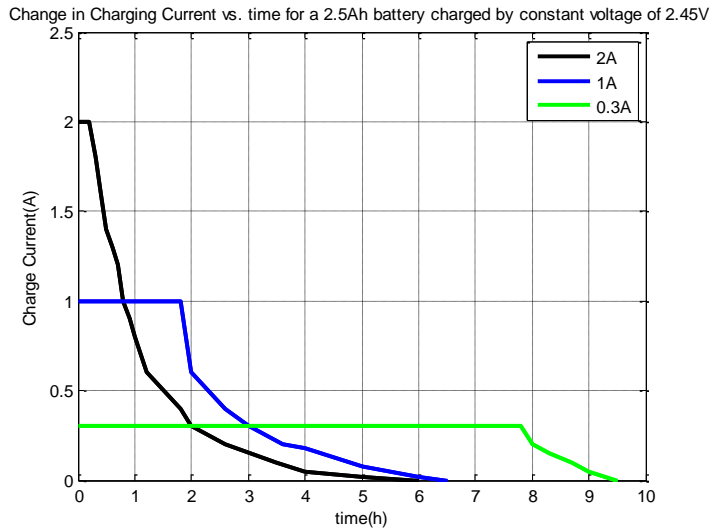


Figure 5. Charge Current vs. Charging Time for three different current limits (Linden et al. 2002)

From the Figure 5, it can be observed that the amount of time to recharge the battery is varied for different current limits. The battery charging process is started with a constant current for different charging currents. When the battery voltage is reached the gassing voltage (threshold) the charging current starts to drop. The only difference between those three charging limits is the amount of time needed to recharge the battery.

In this MSc. Thesis project, Hyperion AC/DC EOS0606iAD-C battery charger is used. The Hyperion has charge, discharge and storage modes. “Pb” Mode is used to select lead-acid batteries in Hyperion and charging current is chosen 300mA. 6 series-connected cells are charged at the same time due to the specifications. Therefore, total battery voltage is chosen 12V. The most important specifications of Hyperion AC/DC EOS0606iAD-C battery charger is given in Table 1.

Table 1. Specifications of Hyperion AC/DC EOS0606iAD-C (Hyperion)

Input voltage range	11-15V DC
Range of series-connected lead-acid battery cells	1-6
Charge current	100mA ~ 6A max. by 100mA steps for lead-acid batteries
Charge termination	CV/CC for lead-acid batteries

The Hyperion AC/DC EOS0606iAD-C battery charger is shown in Figure 6.



Figure 6. Hyperion AC/DC EOS0606iAD-C battery charger (Hyperion 2013)

2.3.3. Comparison of Rechargeable Batteries

In this part, the characteristics and advantages/disadvantages of lead-acid batteries compared to other rechargeable battery types are explained.

Table 2. Characteristics of different rechargeable batteries (Pistoia 2005)

Characteristics/Cell	Lead-Acid	Li-ion	Ni-MH	Ni-Cd	Alkaline
Specific Energy (Wh/kg)	30 to 50	150 to 190	60 to 90	40 to 60	80
Fast Charge Time (h)	8 to 16	2 to 3	1	1	2 to 3
Overcharge Tolerance	high	very low	low	moderate	moderate
Self-Discharge (%/month)	5	<5	30	20	0.3
Nominal Cell Voltage (V)	2	3.7	1.25	1.25	1.5
Operating Temperature (°C) (only discharge)	-20 to 60	-20 to 60	-20 to 60	-40 to 60	0 to 65

Hence, it can be observed from the Table 2 that lead-acid batteries have different characteristics over other rechargeable batteries. According to Linden et al. (2002), the advantages and disadvantages of lead-acid batteries are given in the Table 3:

Table 3. *Advantages and disadvantages of lead-acid batteries compared to other rechargeable battery types (Linden et al. 2002)*

Advantages	Disadvantages
Widely used and manufactured globally	The energy density (Wh/kg) is low
Good performance in at low and high temperatures	Hard to be produced in small sizes
High electrical turnaround charge efficiency (70% ~ 80%) which compares outward discharge energy with inward charge energy	Not possible to store in discharged condition
High nominal cell voltage (but less than Li-Ion)	Wheeled and stationary usage is limited
High overcharge tolerance	Thermal runaway can occur if the charging is not proper
Explicit SoC demonstration	Transportation limitations
Less maintenance need	Depending on number of cells, the battery pack might be heavy

According to Broussely et al. (2007) and Pistoia (2009), the characteristics of lead-acid batteries are given in the Table 4. Note that the Enersys Cyclon D Cell Sealed lead-acid batteries are used in our PMU project. The recommended EODV (end of discharge voltage) with respect to the discharge rate is given in table in Appendix 3.

Table 4. *Characteristics of Lead-Acid Batteries (Broussely et al. 2007 & Pistoia 2009)*

Lead-Acid System (Application Areas)	Voltage Range (Float) (V)	Operating Temperature(°C)
Sealed	1.8 to 2	-40 to 60
SLI (starting lighting ignition) (cars, aircrafts, ships)	1.8 to 2	-40 to 55
Traction (electric trucks, road vehicles)	1.8 to 2	-20 to 40
Stationary (telecommunications, UPS, energy storage)	1.8 to 2	-10 to 40
Cyclon D Cell Sealed	1.93 to 2.14	-65 to 80

It can be concluded from Table 4 that, “Cyclon D Cell Sealed” lead-acid batteries have different float voltage range than other types of lead-acid batteries. Furthermore, the operating temperature range of “Cyclon D Cell Sealed” lead-acid batteries is higher than other types of lead-acid batteries. Cyclon D Cell Sealed lead-acid batteries can be used in telecommunications, UPS, energy storage, electric vehicles, solar power equipments, aerospace, etc. Therefore, from all reasons above the “Cyclon D Cell Sealed” lead-acid batteries are used in our PMU project. In addition, the capacity of Cyclon D Cell Sealed-Lead rechargeable 2V battery is equal to 2.5Ah.

2.3.4. Future of Lead-Acid Batteries

According to Clarke (2011); cheap expansion, manufacturing scale and 100% recycling of lead-acid batteries have a key role in fast growing battery markets. In addition, lead-acid batteries should satisfy the energy density requirement of Li-ion batteries in future. Moreover, lead-acid batteries may have less charging time, higher life cycle and more direct current path to gain advantage over other batteries found in the industry.

Furthermore, the manufacturing process steps and the materials or equipment that used in lead-acid batteries can be reduced.

2.4. State of Charge (SoC) Calculations

SoC estimation is a crucial indicator for managing batteries and providing reliable operations for them. It shows the amount of energy remained in the battery. It prevents unpredictable and unwanted energy loss of the battery system. It also demonstrates if the battery cell is overcharged or not. Hence, it provides a longer life for batteries (Kong-Soon et al. 2008).

2.4.1. The SoC Calculation Methods

There are different ways to calculate SoC of lead-acid batteries. One solution method for lead-acid battery SoC estimation is presented by Pang et al. (2001). The approach of Pang et al. (2001) to calculate SoC of lead-acid batteries is based on estimating the open circuit voltage (OCV) of the lead-acid battery and then providing a linear relationship between OCV and SoC.

According to Pang et al. (2001):

$$SoC = \frac{OCV - \beta}{\alpha} \quad (1)$$

where β is the lead-acid battery terminal voltage when SoC is equal to 0% (when lead-acid battery charge is drained) and α is obtained via putting the OCV and β values in equation (1) when SoC is equal to 100% (when lead-acid battery is fully charged).

Additionally, the relation between Cyclon cell voltages and SoC is based on the Figure 7. According to Enersys Cyclon (2008), SoC of Enersys Cyclon battery can be calculated using the curve given in the Figure 7.

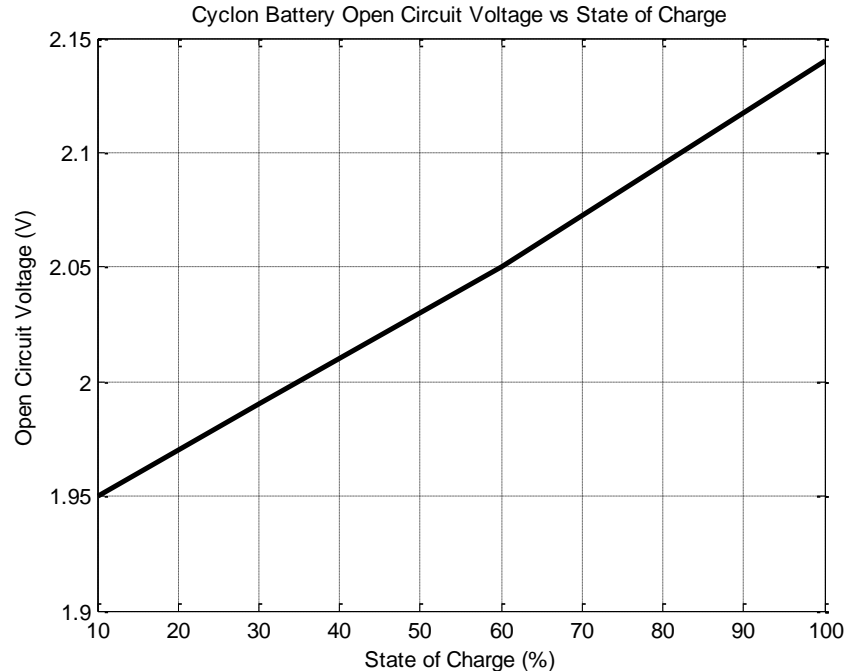


Figure 7. Enersys Cyclon Battery Open Circuit Voltage vs. State of Charge (Enersys Cyclon 2008)

The Figure 7 is valid to within 20% of correct SoC of battery cell, if the cell has not been applied any charge/discharge operations within the last 24 hours. In addition, the Figure 7 is valid to within 5% of correct SoC of battery cell, if the cell has not been applied any charge/discharge operations within the last 5 days. Therefore, the open circuit voltage (OCV) of lead-acid batteries is dependent of charging/discharging rates and the amount of time they have been disconnected from charger.

The Cyclon battery should have the required overcharge to reach long battery life. Under proper charging conditions the Figure 7 is valid for ten years (Enersys Cyclon 2008). The proper charging method for Cyclon batteries is Constant Current/Constant Voltage (CC/CV) method which is explained in section 2.3.2.1.

Furthermore, it is observed from the Figure 7 that the SoC of lead-acid battery is a linear function of open circuit voltage. The battery cell is considered as fully charged when the OCV is greater than **2.14 V/cell** and fully discharged when the OCV is less than **1.94 V/cell**. The relationship between OCV and SoC of a lead-acid battery cell is given in the Table 5.

Table 5. *Open Circuit Voltage vs. State of Charge of lead-acid battery cell*

OCV (V)	SoC (%)
>2.14	100
(2.13-2.14]	95
(2.12-2.13]	90
(2.11-2.12]	85
(2.1-2.11]	80
(2.09-2.1]	75
(2.08-2.09]	70
(2.07-2.08]	65
(2.05-2.07]	60
(2.04-2.05]	55
(2.03-2.04]	50
(2.02-2.03]	45
(2.01-2.02]	40
(2-2.01]	35
(1.99-2]	30
(1.98-1.99]	25
(1.97-1.98]	20
(1.96-1.97]	15
(1.95-1.96]	10
(1.94-1.95]	5
<1.94	0

According to the Table 5, the lead-acid battery cell reaches 100% SoC if the voltage level of that cell is greater than 2.14V.

2.5. State of Health (SoH) Estimations

Battery SoH is an important estimation to observe the battery performance. According to Tanaami et al. (2009), SoH estimations show how much the battery can supply its maximum capacity under usual charging or discharging conditions. The battery aging comes up when the charge and discharge cycles of a rechargeable battery are increased. In addition, the battery aging can occur if the battery is used improperly during charging or discharging. The battery aging is an important reason to affect battery life and capacity.

According to Huet (1998), the charging or discharging current magnitude, DoD (depth of discharge), room temperature, battery charge control method, over charging or discharging, storage type and duration are the factors that affect the battery SoH.

An early breakdown of the lead-acid battery of the device can cause a problem since the electrical power consumption of that device is increasing by the time of progress. Hence, the battery SoH estimation is crucial and required for devices during the

process. The Gas Gauge Algorithm can be used to estimate SoH. The equations of Gas Gauge Algorithm to estimate SoH are given in following equations step by step (Texas Instruments 2006).

$$DoD = 1 - SoC \quad (2)$$

Simply, the depth of discharge given in the equation (2) is the complement of state of charge. The gas gauge updates data on DoD based upon OCV (open circuit voltage) readings during a relaxed mode for each cell individually (Texas Instruments 2006). As it is illustrated in figure given in Appendix 4, the subsequent DoD measurements are taken when 30 minutes elapsed in the relaxation mode. After that DoD measurements are taken every 100 seconds.

$$Q_{passed} = |Q_1 - Q_2| \quad (3)$$

where Q_1 is the first passed charge from the fully charged state and similarly Q_2 is the second passed charge from the fully charged state. Q_{passed} is set to zero for every DoD_0 update.

$$Q_{max} = \frac{Q_{passed}}{|SoC_1 - SoC_2|} \quad (4)$$

where

$$SoC_1 = \frac{Q_1}{Q_{max}} \quad (5)$$

and similarly

$$SoC_2 = \frac{Q_2}{Q_{max}} \quad (6)$$

In the equation (4), Q_{max} denotes the maximum capacity of the battery has. Q_{max} is updated when:

$$\frac{dV}{dt} < 4\mu V / s \quad (7)$$

The equation (7) denotes the rate of instantaneous voltage change over time (volts per second). As it is obtained from the figure given in Appendix 4, Q_{max} is also updated when the maximal time is exceeded.

$$RM = (DoD_{final} - DoD_{start}) \times Q_{max} \quad (8)$$

Thus, the Gas Gauge Algorithm utilizes DoD and Q_{max} (total chemical capacity) informations to estimate the RM (remaining capacity).

$$FCC = Q_{start} + Q_{passed} + RM \quad (9)$$

where Q_{start} denotes the passed charge which makes DoD equal to DoD_0 . Q_{start} is equal to zero for a fully charged battery. DoD_0 stands for the last DoD reading before charging or discharging. FCC (full charge capacity) is the passed charge quantity from fully-charged condition to the system termination voltage. The passed charge must be higher than 37% of design capacity to allow the occurrence of an update. In other words,

FCC is the available capacity at the present charging or discharging rate. FCC depends on the temperature at a time of measurement and load.

Consequently, the formula to calculate SoH is given in the equation (10) (Williams 2012):

$$SoH = \frac{FCC}{Design\ Capacity} \quad (11)$$

In brief, the SoH monitors the chemical degradation and shows when the battery should be replaced.

3. SYSTEM CONSIDERATIONS BASED ON MAX11068

The system considerations given in this chapter describe MAX11068 which is used in this Smart Battery Power Management Unit (PMU) project.

3.1. Inter-Integrated Circuit (I²C) Communication

I²C is a multi-master bi-directional 2-wire bus for efficient inter-IC control. Multi-master means more than one device capable of controlling bus can be connected to it. However, only one master is active at any time. It maximizes hardware efficiency and circuit simplicity. Some of crucial features of I²C are listed below (NXP Semiconductors 2012):

- Only serial data line (SDA) and serial clock line (SCL) are required and it is exactly software-defined.
- All I²C-bus compatible devices communicate directly with each other via I²C-bus.
- Masters can run as master-transmitters or as master-receivers. They control the I²C-bus by sending data and addresses.
- It has collision detection, clock synchronization and arbitration properties to block data overlap if two or more masters simultaneously begin data transfer.
- Permits a system to be changed easily by clipping or unclipping ICs (integrated circuits) to or from the bus without affecting any other functions of I²C-bus.
- The I²C-bus interfaces are not required to be changed.

SDA and SCL convey the information between devices that connected to I²C-bus. The devices that connected to I²C-bus have their unique addresses. More importantly, for the PMU projects I²C communication provides very low current consumption, high noise independence and broad range of the supply voltage and temperature.

Table 6. Definition of I²C-bus terminology

Term	Task
Transmitter	Sends data to I ² C-bus
Master	Begins a transfer, creates clock signals and ends a transfer
Synchronization	Synchronizes clock signals of more than one device
Arbitration	If more than one master simultaneously attempts to control I ² C-bus, only one is supposed to do so the other master loses the arbitration and waits until it is allowed to begin transmission

3.1.1. Serial Data Line (SDA) and Serial Clock Line (SCL)

According to the NXP Semiconductors (2012), the SDA and SCL are both bidirectional. When the I²C-bus is not assigned any job, the SDA and SCL levels are both HIGH ('1').

Since any device which may have metal-oxide-semiconductor (MOS) and bipolar technologies can be connected to I²C-bus, the SDA and SCL levels are not defined as LOW ('0') or HIGH ('1'). The levels depend on positive supply voltage of FET (V_{DD}). The low-level input voltage (V_{IL}) is set as $0.3V_{DD}$ and high-level input voltage (V_{IH}) is set as $0.7V_{DD}$.

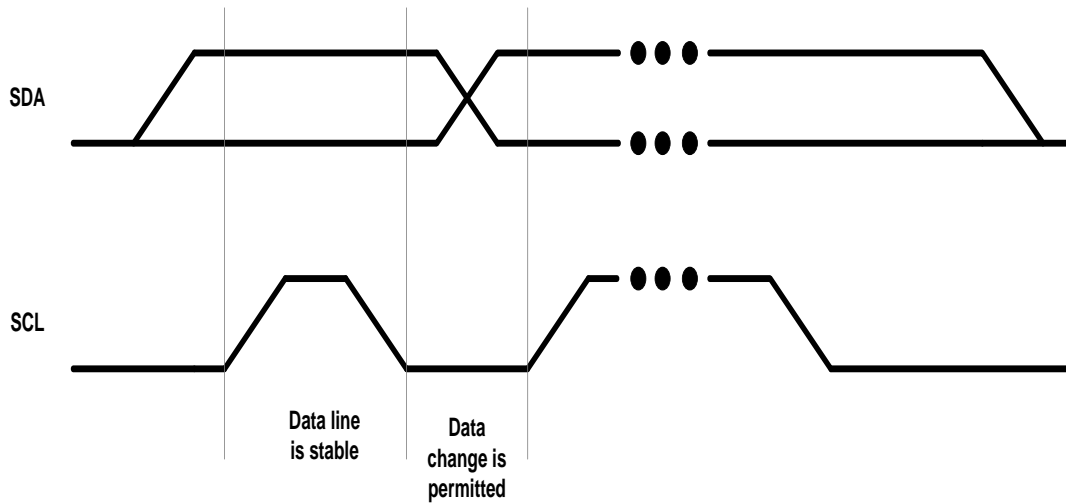


Figure 8. I²C-bus bit transmission (NXP Semiconductors 2012)

From Figure 8 it is obtained that the data on SDA has to be stable when the clock signal is HIGH. Moreover, the LOW or HIGH level of SDA is changed when the SCL clock is LOW. In addition, for each transmitted data bit one clock pulse is produced.

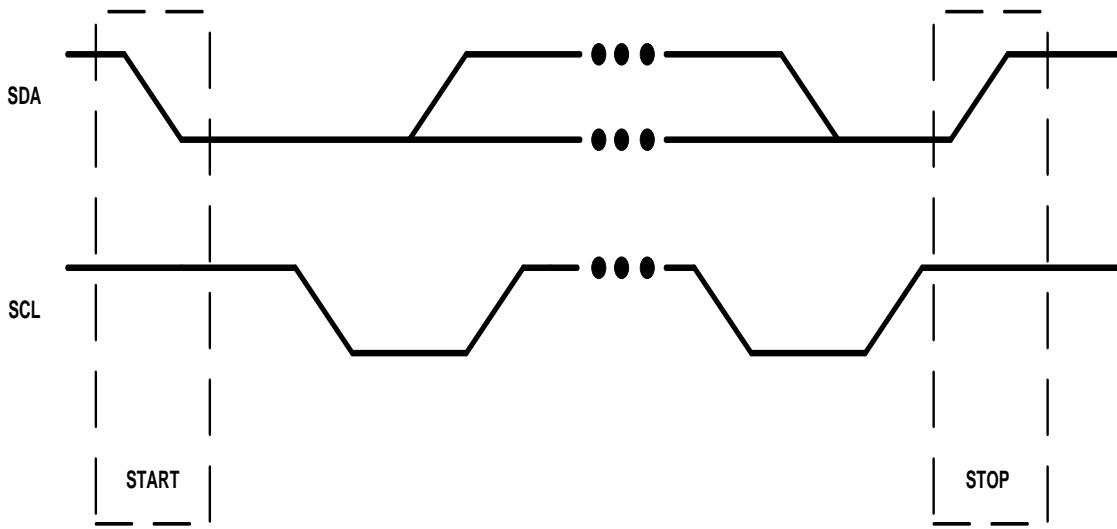


Figure 9. START and STOP conditions (NXP Semiconductors 2012)

All transmissions that are generated by the master begin with START and end with STOP. As observed from Figure 9, for SDA; the START is acquired by a HIGH to LOW passing when SCL is HIGH. On the other hand, for SDA; the STOP is acquired by a LOW to HIGH passing when SCL is HIGH.

Each byte is followed by an acknowledge (ACK) bit. Data transfer is begun by most significant bit (MSB) first. The ACK bit demonstrates that the data byte transmission is done successfully. When ACK is sent, the receiver sets the SDA as LOW. However, the ACK bit does not ensure the data integrity. The negative-acknowledge (NACK) bit is generated if there is no receiver on I²C-bus or the receiver is not able to receive any data byte. When NACK is sent, the receiver sets the SDA as HIGH.

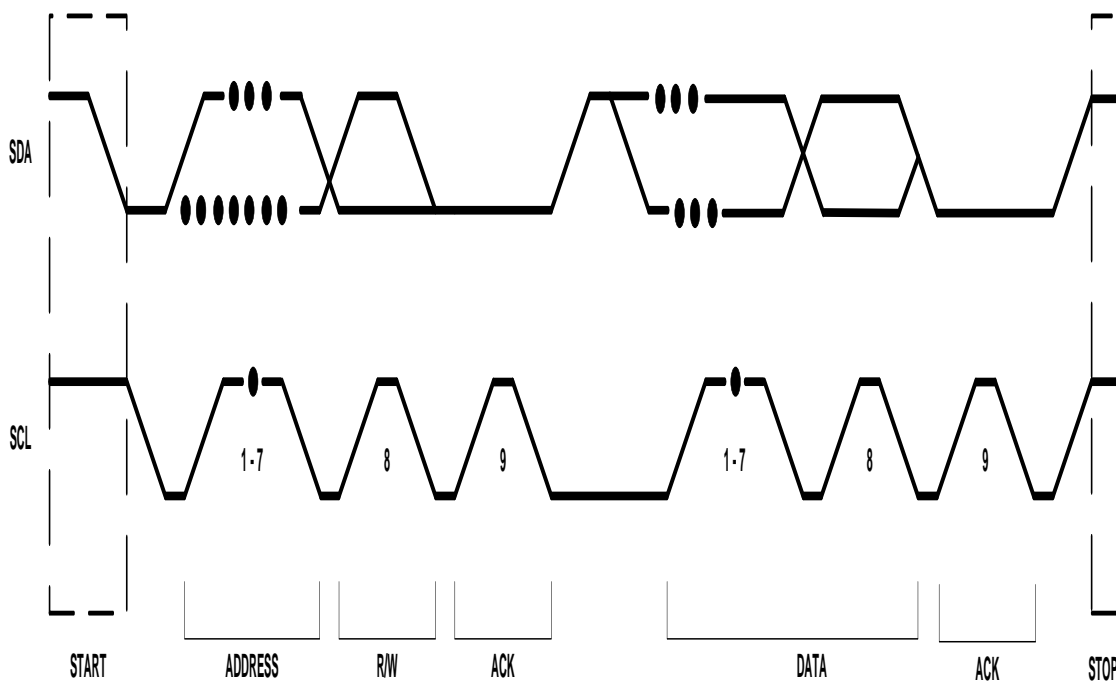


Figure 10. Complete Data Transfer (NXP Semiconductors 2012)

In Figure 10, the slave address is sent after START. The slave address is seven-bits long. It is followed by the read/write (R/W). R/W is a data direction bit. If R/W is zero then the master writes to slave. On the other hand, if R/W is one then the master reads from slave. The data byte transmission is ended by STOP which is generated by the master.

For example, when the master generates a Write, it sends data bits and receives an ACK bit.

If the slaves are slower than masters then the slaves can spread the clock pulse via setting SCL low in a short span of time until it is able to make a new data transmission.

3.1.2. I²C Command List

In the Table 7, the commands together with their functions are given. If the device configuration is addressable, then the initializations given in Table 7 is not used. In addition, Table 7 is specific for the MAX11068.

Table 7. I²C Command List (Maxim Integrated 2010)

Name	Function	PEC Byte
HELLOALL	Setting the all device address via initializing the first device's address in the chain. All other remaining devices are auto-incremented.	Not contain
ROLLCALL	Determining # of devices in the chain.	Not contain
SETLASTADDRESS	Determining which device address is the last one.	Required from the host
WRITEALL	Enabling a value to be written to a register in all active devices at the same time.	Required from the host
WRITEDEVICE	Writing the data to only a certain device.	Required from the host
READALL	Reading the data from a certain device register for all devices in the chain.	Send to the host

According to Maxim Integrated (2010), the first two bits of HELLOALL have to be '1'. Next 5 bits determine the address of first device in system management bus (SMBus) ladder. The last bit is the R/W bit and it must be '0'. The 5-bits starting address is determined as the least significant bit (LSB) is the first bit. The typical starting address is 0x01. Therefore, the HELLOALL command becomes 11100000 in binary format. It is equal to 0xE0 in hexadecimal format.

The ROLLCALL command should be called just after HELLOALL command. When 0xFF is returned it means that the host has addresses of all devices. The ROLLCALL command is a read of address 0x01. The write bit is added at the end of 7-bits broadcast address and it is sent on I²C-bus. Next to this data, the command of address 0x01 register is sent.

The SETLASTADDRESS command is called after ROLLCALL command. The write bit is added at the end of 7-bits broadcast address and it is sent on I²C-bus. Next to this data, the command of address 0x01 register is sent. After that two data bytes are

written to each device which is sent on I²C-bus. The first data byte may be any value. However, the second data byte is written to address register of all devices. Thereafter the PEC (packet-error checking) byte is sent. PEC byte is calculated from first four bytes.

The WRITEALL command is called after SETLASTADDRESS command. The write bit is added at the end of 7-bits broadcast address and it is sent on I²C-bus. Next, the command of address is sent with MSB first. The lower and upper data bytes are added to the data, respectively. After the PEC byte is sent. The PEC byte is calculated from first four bytes.

The WRITEDevice command is called after WRITEALL command. The only difference of WRITEDevice and WRITEALL command is the address byte of I²C-bus of WRITEDevice command has fixed MSBs (0b10 in binary format), pursued by the command of address is sent with LSB first in the place of broadcast address.

The READALL command is called after WRITEDevice command. The write bit is added at the end of 7-bits broadcast address and it is sent on I²C-bus. Next to this data, the command byte is sent. To change the direction of bit stream, the repeated start (SR) is sent. On the contrary, this time the read bit is added at the end of 7-bits broadcast address instead of the read bit and it is sent on I²C-bus.

In Table 8, the address bits of commands are shown. The Broadcast Address is used for ROLLCALL, WRITEALL and READALL commands.

Table 8. I²C-bus Address Bits (Maxim Integrated 2010)

Command	7	6	5	4	3	2	1	R/W
Broadcast Address	B7	B6	B5	B4	B3	B2	B	1/0
(Default)	0	1	0	0	0	0	0	1/0
HELLOALL	1	1	A0	A1	A2	A3	A4	0
WRITEDevice	1	0	A0	A1	A2	A3	A4	0

In the Smart Battery PMU project the PEC bytes are calculated via Pseudo-Code Algorithm for a CRC-8 PEC Calculation (Maxim Integrated 2010). MAX11068 utilizes SMBus PEC algorithm to sustain the completeness of data. The CRC-8 algorithm supports SMBus PEC mechanism to carry out calculations. The CRC-8 polynomial ($C(x)$) is shown below:

$$C(x) = x^8 + x^2 + x + 1$$

At first, $C(x)$ is initialized to zero. The byte is XORed (exclusive ORed) with $C(x)$ for each input byte and called as ‘Remainder’. When MSB is equal to one then the remainder is left-shifted and XORed with eight LSBs of the $C(x)$. When MSB is equal to zero then the remainder is left-shifted by one bit. This is applied until eight left-shifts are acquired. Next, the transaction is repeated on the next input byte using current $C(x)$. When the process of all input bytes is completed the last result is the output byte of $C(x)$.

Consequently, MAX11068 gets functional after any reset event. In Figure 11, the complete functional I²C SMBus ladder communication initialization sequence diagram of MAX11068 is shown. The SMBus ladder modules are set for operation after they are regulated for communication.

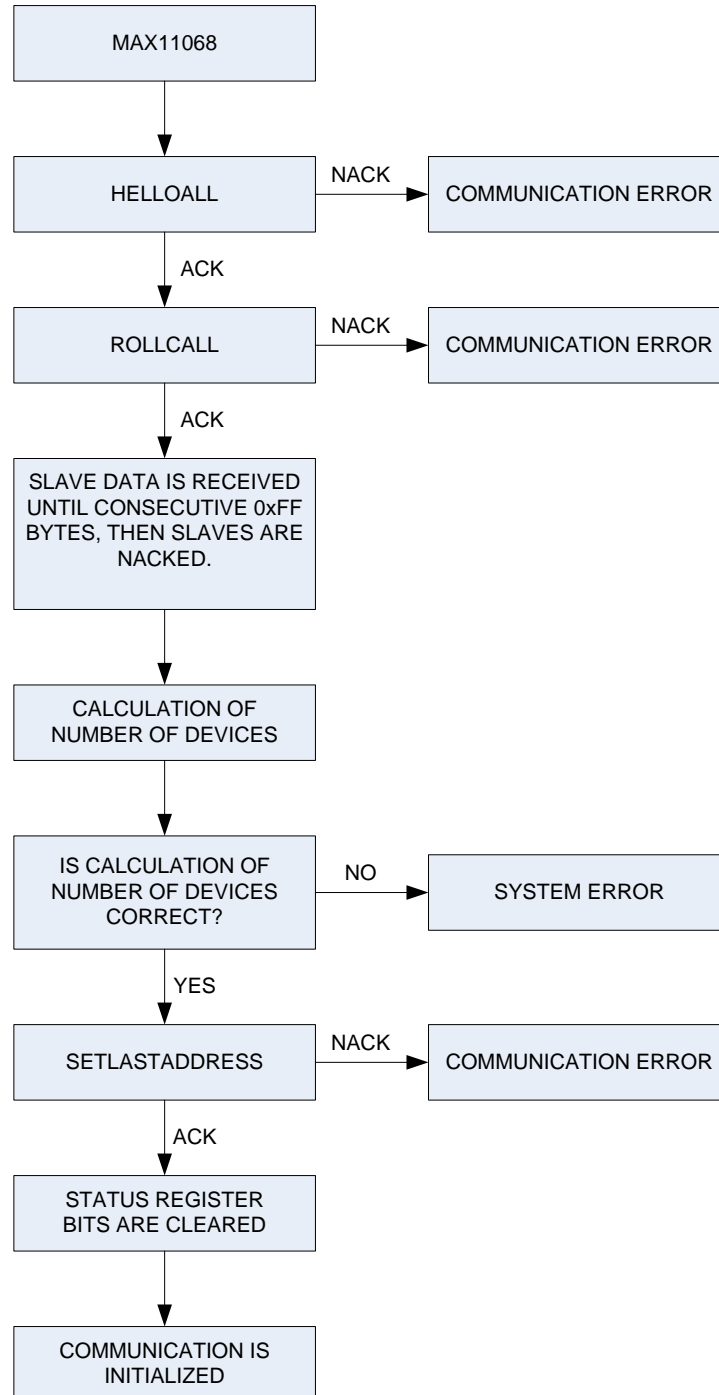


Figure 11. Functional Communication Initialization Sequence Diagram of MAX11068
(Maxim Integrated 2010)

3.2. MAX11068

The MAX11068 integrated battery sensor is used for managing the lead-acid batteries in this MSc. Thesis. The BMS topology is master-slave architecture in MAX11068. The MAX11068 can measure the voltage of up to 12 cells and has two auxiliary ports which can be used with thermistors for temperature measurements. Moreover, the MAX11068 evaluation kit (EVKit) can measure the voltage of up to hundreds of cells depending on the battery selection. In Figure 12, Functional Block Diagram of MAX11068 is illustrated (Maxim Integrated 2010).

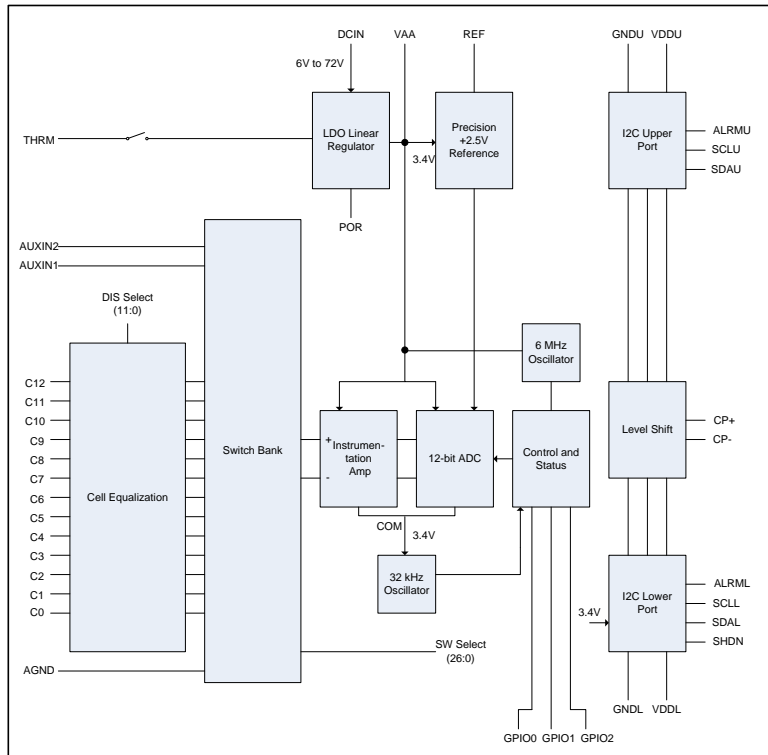


Figure 12. Functional Block Diagram of MAX11068 (Maxim Integrated 2010)

In Figure 12, cell data is obtained by consecutive approximation of 12-bit analog-to-digital converter (ADC). It also enables to measure internal and external temperature. The switch bank results from a high voltage multiplexer. It forms switching between the cells. When cells are switched; the cells are measured by the 12-bit ADC and after that they are stored in internal memory. All cells are measured with 2.5V voltage reference for gaining high accuracy. Internal switch can be used to charge a cell slower than other cells if that cell has higher voltage than the other cells. The whole MAX11068 is controlled by the 6MHz internal oscillator. It determines the communication speed and ADC operations. I²C Upper Port (master port) is level shifted and referenced to ground (GND_U).

MAX11068 is a programmable battery-monitoring data collection IC whereas MAX11080 is a battery pack fault monitor IC. The MAX11068 monitor measures battery parameters (voltage, temperature, State of Charge (SoC), State of Health (SoH), etc.) including the control loop. It controls indirectly the charger and the load. A monitor cannot interrupt the pack current (Maxim Integrated 2010). The balancer maximizes the pack performance via providing cell balancing. The balancer is sufficient for the BMS as long as it can control the charger and the load. The MAX11080 IC only checks for under/over voltage and temperature. It cannot monitor the SoC or SoH. The fault signal of the MAX11080 is not used in this MSc. Thesis. From Figure 13, the MAX11068 EVKit can be seen.

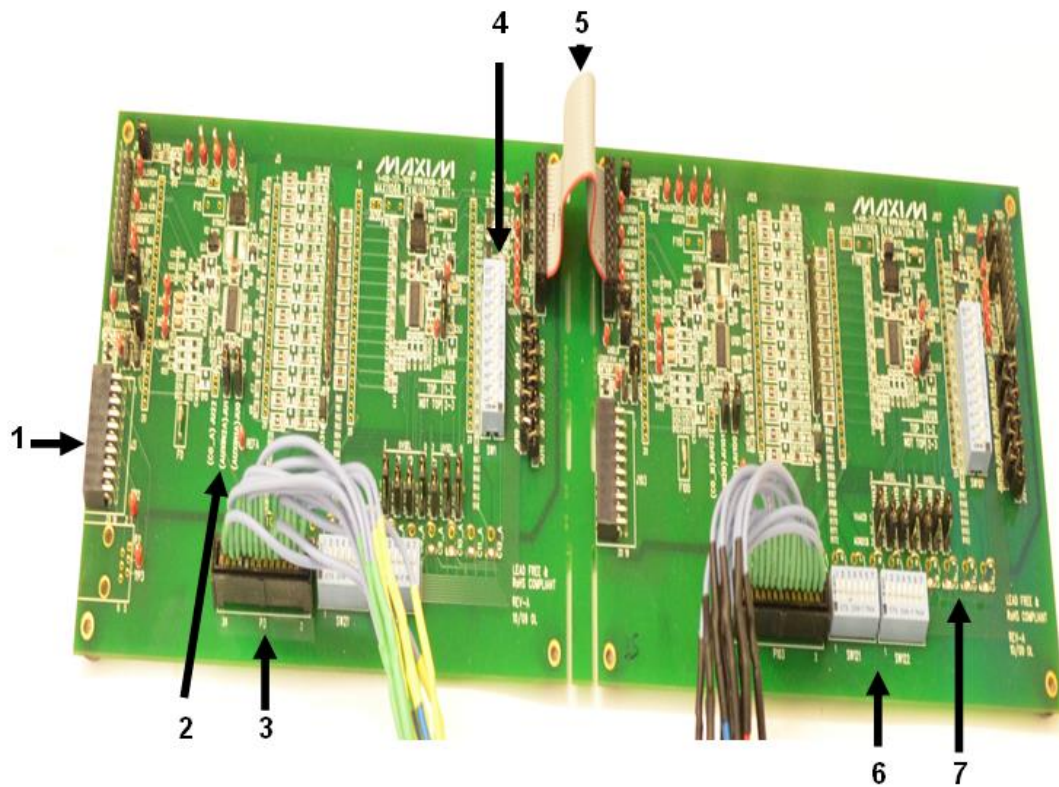


Figure 13. MAX11068 EVKit (Maxim Integrated)

The numbers given in Figure 13 denotes that:

1. Arduino Connection Header
2. Auxiliary Inputs
3. Header that is connected to battery cells
4. Cell configuration switch
5. Ribbon cable that connect two MAX11068 EVKits
6. Switch that switches the battery cells in and out of BMS
7. Cell stack voltages

3.2.1. Analog-to-Digital Converter (ADC)

The MAX11068 can measure 12 cells. A 12-bit ADC is utilized to digitize the cell voltages. The MAX11068 measures each cell differentially. The MAX11068 has a measurement range from 0 to 5V (Maxim Integrated 2010).

The output of ADC shows the cell measurement result. The following equation is used to calculate the cell voltage.

$$Cell\ Voltage = \frac{ADC(out) \times 5}{4096}$$

In the equation above, the 4096 comes from 2^{12} since the maximum data bits are equal to 12. In addition the $ADC(out)$ is multiplied by 5 because the maximum cell voltage measurement could be equal to 5V.

3.3. Jumper/Switch Configurations and Cell Connections

Table 9 provides the complete shunt positions for the MAX11068 evaluation kit (EVKit). The Tables 9 and 10 are done according to Maxim Integrated MAX11068 Evaluation System (2010).

Table 9. Jumper Configurations based on number of cells of MAX11068 EVALUATION KIT+ PACK A & B

# of Cells	Position of Shunt									
	JU2, JU102	JU3, JU103	JU4, JU104	JU5, JU105	JU6, JU106	JU7, JU107	JU8, JU108	JU9, JU109	JU10, JU110	JU11, JU111
2	On	On	On	On	On	On	On	On	On	On
3	Off	On	On	On	On	On	On	On	On	On
4	Off	Off	On	On	On	On	On	On	On	On
5	Off	Off	Off	On	On	On	On	On	On	On
6	Off	Off	Off	Off	On	On	On	On	On	On
7	Off	Off	Off	Off	Off	On	On	On	On	On
8	Off	Off	Off	Off	Off	Off	On	On	On	On
9	Off	Off	Off	Off	Off	Off	Off	On	On	On
10	Off	Off	Off	Off	Off	Off	Off	Off	On	On
11	Off	Off	Off	Off	Off	Off	Off	Off	Off	On
12	Off	Off	Off	Off	Off	Off	Off	Off	Off	Off

As 12 cells are used for each MAX11068 Evaluation Kit+ Pack in our Smart Battery PMU project, the shunts given in Table 9 should be positioned off. Moreover, the cell stack voltage is ensured by cascading 12 battery cells between C0_A to C12_A and C0_B to C12_B nodes. In addition to Table 10, for MAX11068 EVALUATION KIT+ PACKB; header P103 has same cell connections as P3.

Table 10. Header P3 Cell Connections of MAX11068 EVALUATION KIT+ PACKA

CELL #	+TERMINAL	-TERMINAL
1	P3-2	P3-4
2	P3-4	P3-6
3	P3-6	P3-8
4	P3-8	P3-10
5	P3-10	P3-12
6	P3-12	P3-14
7	P3-14	P3-16
8	P3-16	P3-18
9	P3-18	P3-20
10	P3-20	P3-22
11	P3-22	P3-24
12	P3-24	P3-26

3.4. Starting up the MAX11068 EV kit

After applying at least 6 Volts across MAX11068 EVALUATION KIT+ PACKA+ and PACKA-, $\overline{\text{SHDNINA}}$ net should be droved high. In our project, we control SHDNINA by our software. To do this, in addition to the Table 10, the jumpers and switches should be configured as in the Table 11 according to the Maxim Integrated MAX11068 Evaluation System (2010).

Table 11. Jumper Configurations of MAX11068 EVALUATION KIT+ PACK A & B

Jumper	Position of Shunt
JU0, JU100	On
JU1, JU101	On
JU12, JU112	Off
JU13, JU113	1-2
JU14, JU114	2-3
JU15, JU115	2-3
JU16, JU116	1-2
JU17, JU117	2-3
JU18, JU118	1-2
JU19, JU119	1-2
JU20, JU120	On
JU21, JU121	Off
JU24, JU124	On
JU25, JU125	On
JU26, JU126	On
JU28	2-3
JU128	1-2
JU31, JU131, JU32, JU132	On

Jumpers JU0, JU1, JU100 and JU101 enable or disable the auxiliary inputs to measure external resistance temperature detector (RTD) components (Maxim Integrated MAX11068 Evaluation System 2010). The negative temperature coefficient (NTC) RTD can be structured with auxiliary analog inputs to measure battery cell temperature. Since the temperature measurement of battery cells is not a part of our PMU project, the auxiliary inputs are not used via installing a shunt on jumpers JU0, JU1, JU100 and JU101. The cell configuration switch SW101 is given in Appendix 1 and the cell connection switches are given in Appendix 2.

Table 12. *Switch Configurations of MAX11068 EVALUATION KIT+ PACK A & B*

Switch	Switch Position
SW1, SW101	Off
SW21, SW22, SW121, SW122	On

After the all configurations, using a universal serial bus (USB) cable; the MAX11068 Evaluation Kit+ Pack A is connected to personal computer (PC) via Arduino Due. Arduino Due is connected to MAX11068 Evaluation Kit+ Pack A's J3 header.

Table 13. *J3 Header Pinout of MAX11068 EVALUATION KIT+ PACK A*

Pin Number	Net Association
1	$\overline{\text{SHDNINA}}$
3	SDALA
5	GNDLA
7	SCLLA
9	Not Configured
11	$\overline{\text{SHDNA}}$
13	Not Configured
15	Not Configured
17	Not Configured
2, 4, 6, 8, 10, 12, 14, 16, 18, 19	GNDLA

3.4.1. MAX11068 EVKit SMBus Ladder

MAX11068 Evaluation Kit utilizes I²C communication to cascade up to 31 MAX11068 devices via routing I²C communication to headers J1 & J2 for Board (A) and J101 & J102 for Board (B). Since one shipped MAX11068 Evaluation Kit involves two boards (boards A & B), 16 MAX11068 Evaluation Kits are required to acquire 31-device SMBus ladder (Maxim Integrated MAX11068 Evaluation System 2010).

In Figure 14, the MAX11068 EVKit SMBus Ladder can be found when Board (A) is the first board (Maxim Integrated MAX11068 Evaluation System 2010).

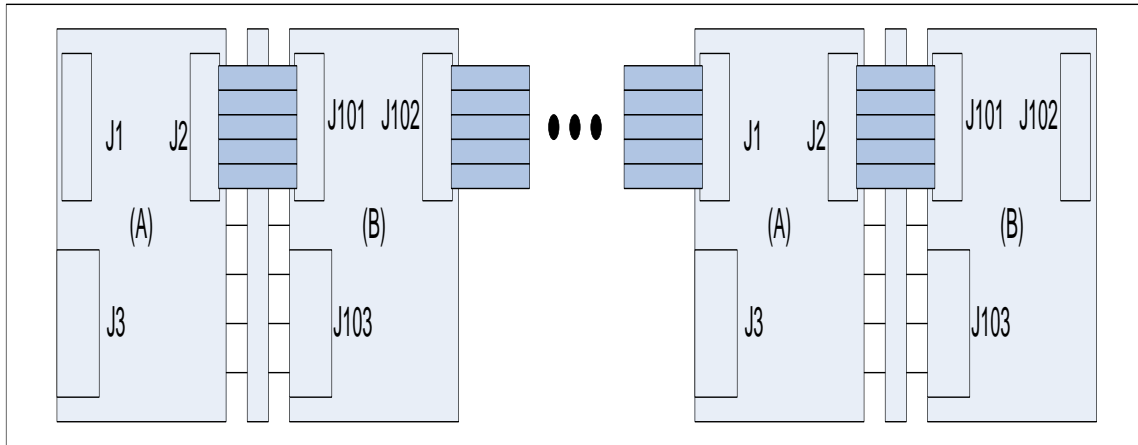


Figure 14. MAX11068 EVKit SMBus Ladder when Board (A) is first board (Maxim Integrated MAX11068 Evaluation System 2010)

In the Smart Battery PMU project two MAX11068 boards (boards A & B) are used. They are connected via ribbon cable that placed across the jumpers J2 and J101. Furthermore, the cell configuration headers J101 and J102 are given in Appendix 1.

Table 14. J1 Header Pinout of MAX11068 EVALUATION KIT+ PACK A

Pin Number	Net Association
1	SHDNA
3	SCLLA
5	SDALA
7	ALRMLA
9, 10, 11, 12	CO_A
13	SHDNINCA
15, 17	Not Configured
19	ALRMOUTCA
2, 4, 6, 8	GNDLA
14, 16, 18, 20	AGNDCA

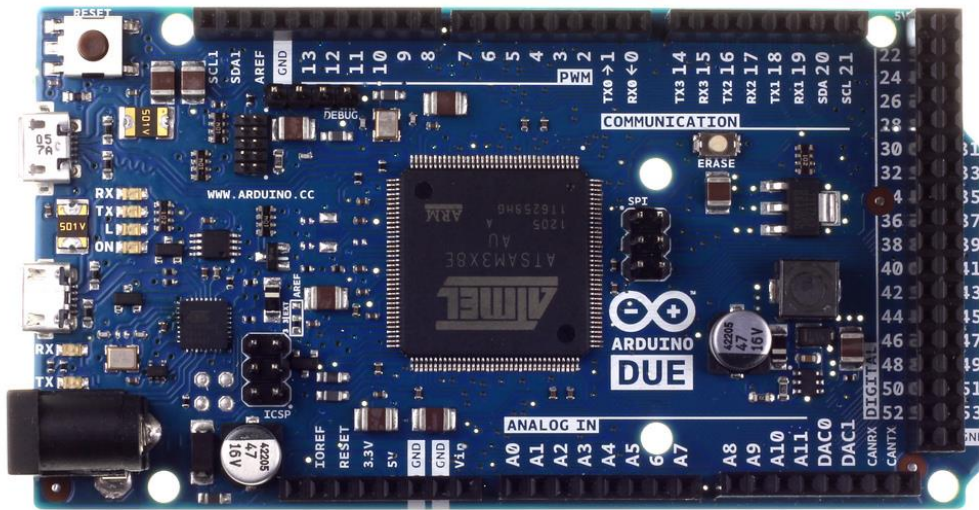
Table 15. J2 Header Pinout of MAX11068 EVALUATION KIT+ PACK A

Pin Number	Net Association
1	CP+A
3	SCLU_A
5	SDAU_A
7	ALRMU_A
9, 10, 11, 12	C12_A
13	CP+CA
15, 17	Not Configured
19	ALRMINCA
2, 4, 6, 8	GNDU1
14, 16, 18, 20	GNDU2

3.5. Arduino Due

The Arduino Due is chosen for this MSc. Thesis. Arduino Due is a microcontroller board which has Atmel SAM3X8E 32-bit ARM chip (Atmel) on it. The Arduino Due has 54 digital pins and each of them can be utilized as an input or output. Nonetheless, 12 of digital I/O pins can be used as pulse width modulation (PWM) outputs. They operate at 3.3V. The input/output (I/O) pins can tolerate maximum 3.3V. Additionally, the direct current (DC) current for 3.3V pin is 800mA. The programming port of Arduino Due is connected to an ATmega16U2 microcontroller which ensures a virtual communication (COM) port (Arduino).

The Figure 15 shows the front view of Arduino Due. The Arduino Due is connected to PC by micro-USB cable. When data is being transmitted between the PC and Arduino Due, the receiver (RX) and transmitter (TX) light-emitting diodes (LEDs) start to flash (Arduino).

**Figure 15.** The front view of Arduino Due (Arduino)

The MAX11068 already includes the USB-powered command module MINIQUSB together with the EVKit software. The MINIQUSB provides the communication between the MAX11068 EVKit and PC (Maxim Integrated 2008). However, the MINIQUSB and EVKit software system is not modifiable and an improved version of visualization is required for user-friendliness. Therefore, a new modifiable system is needed. The Arduino Due is used in order to satisfy that need. The Arduino Due is programmed based on the Maxim Integrated (2010). The MAX11068 EVKit becomes controllable with the Arduino Due. In addition, a new visual quality is provided via a Java graphical user interface (GUI) which is going to be discussed in “Results and Discussion” chapter.

The Arduino Due mainly controls, measures and records the data. Therefore, the title of whole Battery PMU project is extended as ‘Smart’ Battery PMU. The microcontroller board interfaces with the battery packs via I²C communications.

When the battery cells are charged off-limits, the microcontroller has a feature to switch off the charging process. On the other hand, it can charge the weakest battery cell to provide cell balancing. It can be designed to provide a long-life PMU system.

Furthermore, the maximum and minimum battery cell voltages are controlled simultaneously. If the battery cell voltages drop below desired voltage level, the microcontroller can be programmed to alarm the user via the GUI or a speaker mounted on the MAX11068.

The Arduino Due has two I²C interfaces which are SDA1 & SCL1 and SDA (pin #20) & SCL (pin #21). The lowest MAX11068 device of SMBus ladder (Board A) communicates directly with Arduino Due command module. The other MAX11068 devices in SMBus ladder are communicated with Arduino Due command module through the device below them via level-shifted I²C communication bus.

In Table 16, the pin mapping of Arduino Due that used in smart battery PMU system can be found (Arduino).

Table 16. Pin mapping of Arduino Due that used in system

Pin Number	Net Association
20	SDA
21	SCL
52	Digital Pin 52
53	Digital Pin 53
GND	Ground

3.6. Comparison of Selected BMS Boards

In the Table 17, the EVKits or ICs that can be used for managing lead-acid batteries are given. The Table 17 is done according to Maxim Integrated Evaluation System for the MAX11068 (2013), Maxim Integrated MAX17830 12-Channel, High-Voltage Battery Sensor with Advanced SMBus Ladder and External Cell Balancing (2013), Maxim Integrated MAX11068 12-Channel, High-Voltage Battery Sensor, Smart Data-Acquisition Interface (2010), Maxim Integrated Automotive Product Guide (2012) and Linear Technology LTC6804-1/LTC6804-2 Multicell Battery Monitors (2013).

Table 17. Comparison of Different BMS Evaluation Kits

Properties		MAXIM INTEGRATED		LINEAR TECHNOLOGY
General	Part No	MAX11068 EVKit	MAX17830 EVKit	LTC6804 Demo Board
	Availability	All versions are not recommended for new designs.	Future Product	Available
	Voltage Range (for whole pack without external power)	6V to 1.4kV, approximately (nominal)	9V to 2.48kV, approximately (nominal)	11V to 750V, approximately (nominal)
Cells	Topology	Modular Design: 12 cells/board	Modular Design: 12 cells/board	Modular Design: 12 cells/board
	Series cells, min	4	4	4
	Series cells, max (no isolators)	372	372	192
Balancing	On chip, passive	External resistors are needed	External resistors are needed	External resistors are needed
	External, passive	External resistors and MOSFETs are needed	External resistors and MOSFETs are needed	External resistors and MOSFETs are needed
IC Current Drain	Typical Standby (uA)	75	N/A	35
	Typical Operating (mA)	2	N/A	0.45

	Typical Balance (mA)	250	N/A	N/A
Readings	Voltage measurement accuracy	$\pm 0.25\%$, ≤ 5 mV Offset Voltage	$\pm 0.1\%$	$\pm 0.03\%$
	Cell Volt (V), min	0	0	0
	Cell Volt (V), max	5	5	5
	Temperature measurement	Two auxiliary inputs for 12 cells	Two auxiliary inputs for 12 cells	Two auxiliary inputs for every 12 cells
	Data rate	10 kHz to 200 kHz	N/A	Up to 1 MHz
Cost	EVKit	N/A	N/A	\$150
	IC only	N/A	N/A	\$15.25

First of all, from the Table 17, we obtain that LTC6804 is the best choice, if the designers have not had MAX11068 yet, at the moment to design new Battery Management Systems because it is the only available EVKit or IC.

MAX17830 is Maxim Integrated's second generation (next-generation version of the MAX11068) high-accuracy & high-voltage battery-management solution Maxim Integrated MAX17830 12-Channel, High-Voltage Battery Sensor with Advanced SMBus Ladder and External Cell Balancing (2013). Since it is mentioned MAX11068 will be no longer produced (Maxim Integrated Evaluation System for the MAX11068 2013), MAX17830 could be chosen instead of it for future designs. In our MSc. Thesis project MAX11068 was used as it was produced before and consequently available, and MAX17830 is not available at the moment.

Furthermore, MAX11068 has some advantages as well as some disadvantages over the LTC6804. The voltage range for whole pack without any external power of MAX11068 is greater than LTC6804. Moreover, max series cells of MAX11068 are greater than LTC6804. On the other hand, LTC6804 has more voltage measurement accuracy than MAX11068 and the data rate range of LTC6804 is greater than MAX11068. Therefore, the designers should select the right BMS EVKit based on their requirements.

Apart from these, Texas Instrument's bq34z110 which is a lead-acid fuel gauge can be the other option to monitor and state the SoC and SoH of a battery (Texas Instruments 2012). However, it does not have any balancing and protection solution. Therefore, an additional balancing and protection board is needed. Thus, the functionality of bq34z110 is less than MAX11068.

4. POWER MANAGEMENT SYSTEM DESIGN

The complete measurement system, which is illustrated in Figure 16, is consisted of four major parts:

- One 48V battery pack of series-connected 24 lead-acid cells.
- Two MAX11068 evaluation kits (EVKits)
- Arduino Due
- Constant Current Load

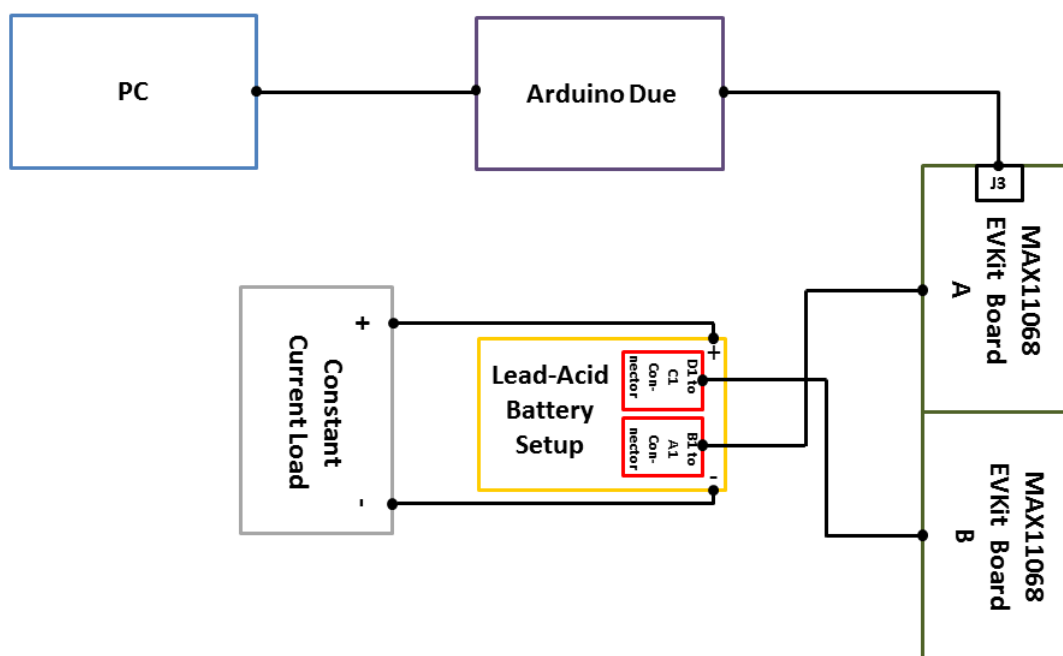


Figure 16. The complete measurement system

The connections of lead-acid battery and Arduino Due to the MAX11068 EVKit are given in Figure 17.

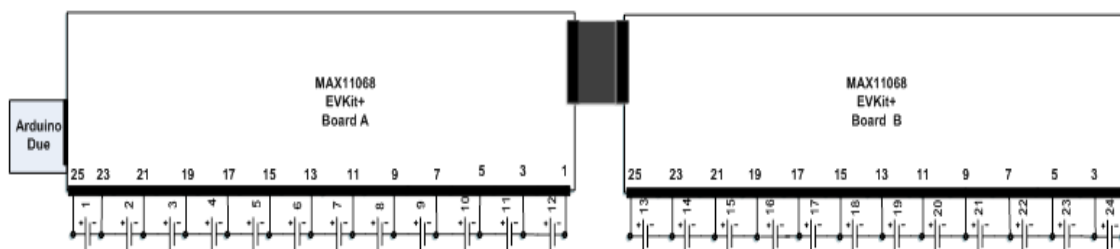


Figure 17. Connection Setup of MAX11068

The series connected 24-cells lead-acid battery design is given in Figure 18.

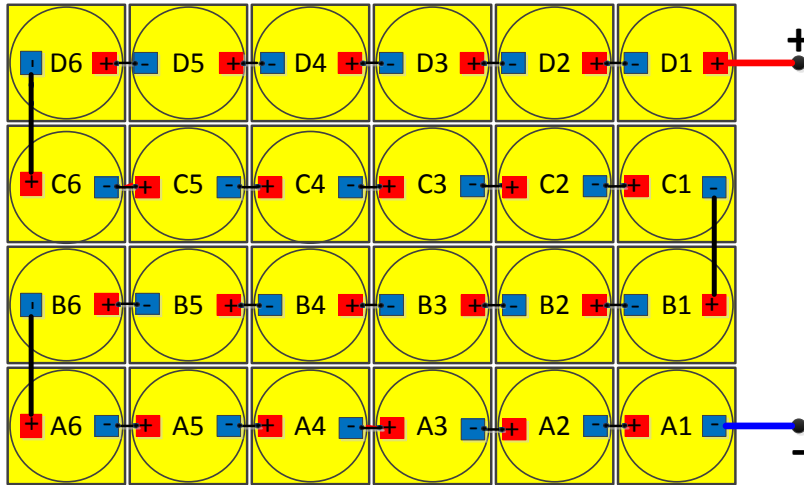


Figure 18. Series connected Lead-Acid battery design

In addition to the wires given in Figure 18, there are also wires which used to connect the battery cells to MAX11068 EVKits.

From the Figure 19, the connection of J3 Header of MAX11068 Evaluation Kit+ PACK A and Arduino Due can be seen. The serial clock line (SCL), serial data line (SDA), faster wakeup (FWUP), backup voltage (VDDBU) and ground (GND) pins of Arduino Due is connected to J3 Header of MAX11068 Evaluation Kit+ PACK A which provides the I²C communication. Since the SHDNINA net should be pulled up to 3.3V (Maxim Integrated MAX11068 Evaluation System 2010), digital pins 52 & 53 of Arduino Due are connected to J3 Header of MAX11068 Evaluation Kit+ PACK A because the input/output (I/O) pins run at 3.3V.

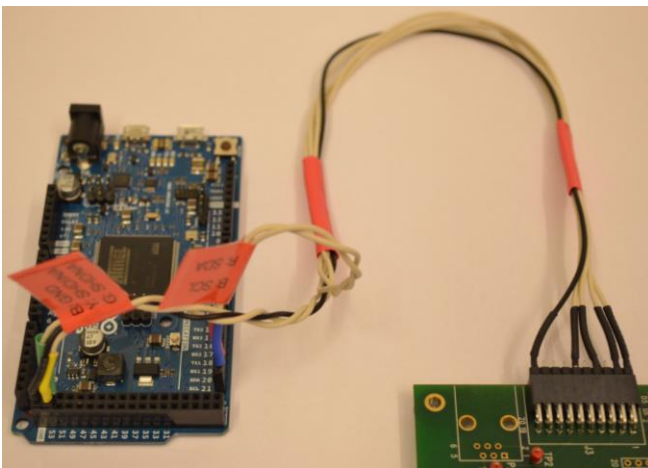


Figure 19. Arduino Due & J3 Header of MAX11068 Evaluation Kit+ PACK A Connection

Furthermore, the constant current load is illustrated in Figure 20. When the voltage is applied on the battery voltage (V_{bat}), the gate resistor (R_G) turns the metal-oxide-semiconductor field-effect transistor (MOSFET) (IRL2910) ON. In addition, the base-emitter voltage ($V_{BE(on)}$) of NPN transistor BC549 is equal to 0.7V. The relationship between the sensing resistor (R_S) and drain current (I_D) is given in the equation (12).

$$R_S = \frac{V_{BE(on)}}{I_D} = \frac{0.7V}{I_D} \quad (12)$$

Hence, I_D is controlled by the R_S value. In the load, R_S is chosen as 0.75Ω . Hence, the constant current through the load is set as approximately 0.9A. When the potential difference between R_S reaches $V_{BE(on)}$, the transistor is turned ON.

The equation for power dissipation of MOSFET (P_D) is given in the equation (13). It is calculated by multiplication of the drain current with potential difference of drain-source.

$$P_D = (V_{bat} - V_{BE(on)}) \times I_D \quad (13)$$

Nonetheless, a big value such as $10k\Omega$ is chosen for R_G so that the transistor is not damaged.

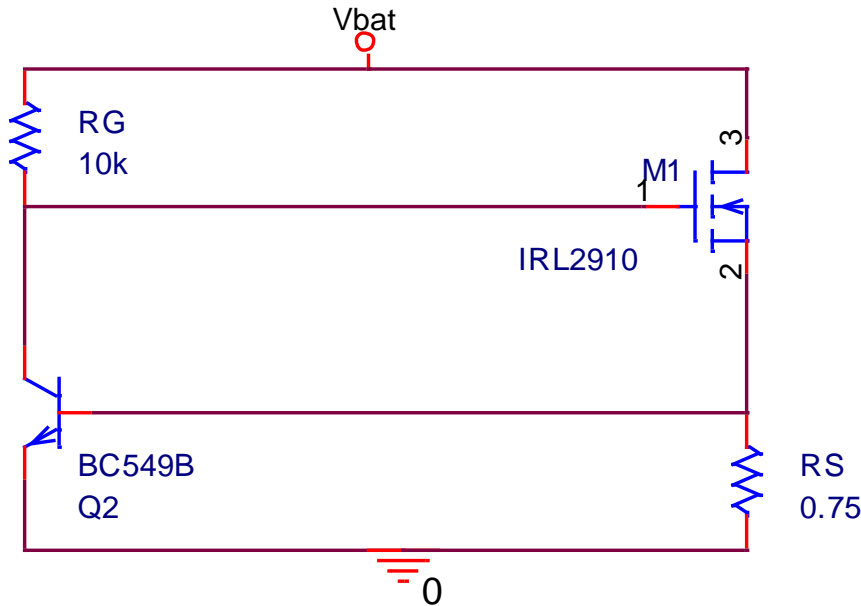


Figure 20. Load design

This constant current load design has some advantages. First, the current can be kept stable independent of battery voltage. Secondly, the R_S dissipates low power since the potential difference across it is nearly 0.7V.

Consequently, with the help of this constant current load, the load discharging curve can be observed.

Lastly, the complete system setup is illustrated in Figure 21.

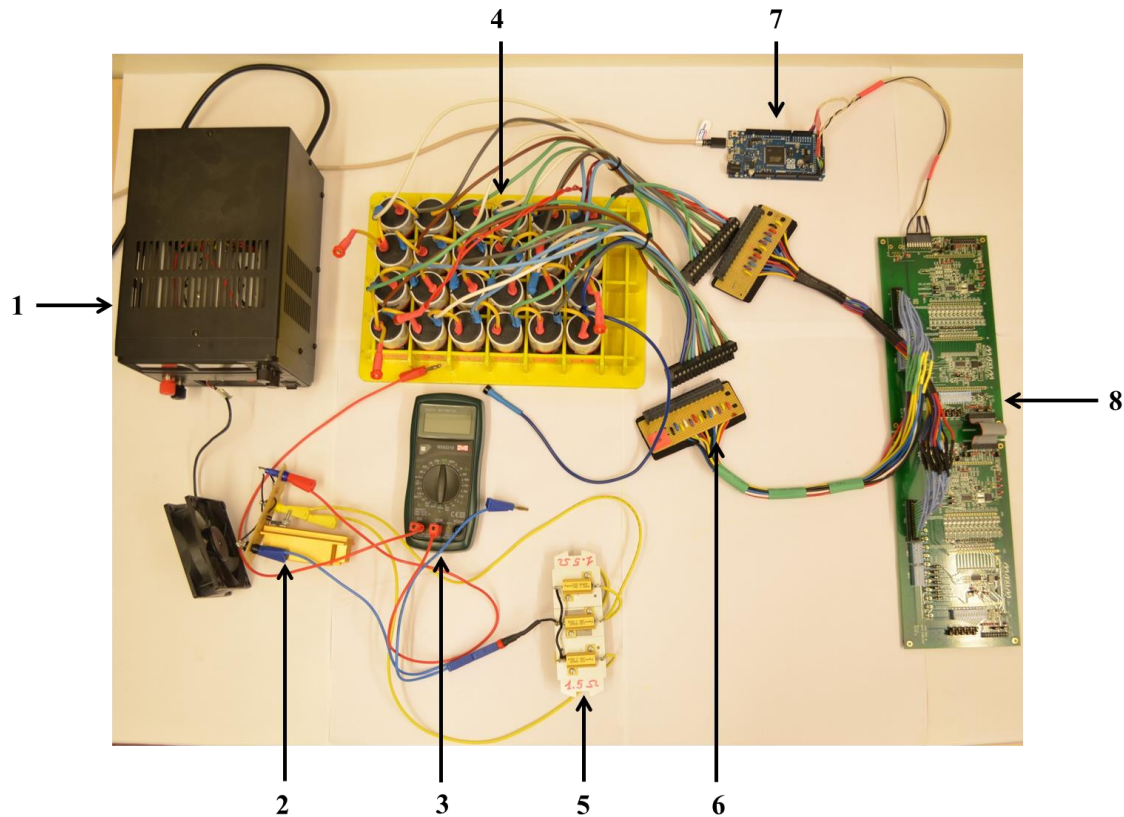


Figure 21. Complete system setup

The numbers given in Figure 21 denotes that:

1. Cooling fan for the MOSFET
2. Constant current load without sensing resistor
3. MS8221D multimeter (Mastech 2013)
4. 24 cells lead-acid battery pack
5. Sensing resistor
6. Connection socket
7. Arduino Due
8. Two MAX11068 EVKits

In the complete system setup, the multimeter is used for measuring the current passing through the load. Also, the connection sockets are connecting two MAX11068 EVKits to the 24 cells lead-acid battery pack. Also, there are two connection sockets for each 12 lead-acid battery cell for the series connected complete 24-cells lead-acid battery setup.

5. PROGRAMMING OF POWER MANAGEMENT UNIT

NetBeans IDE is used for Smart Battery Power Management Unit project. NetBeans IDE is written in one of most widely used programming language, Java (Net Beans 2013).

A Java-based software program, NetBeans IDE, is used in this project for the voltage measurement and display of each battery cell voltage including maximum and minimum voltages of cells of the battery pack and helps to establish a connection with user.

Programming of MAX11068 evaluation kit (EVKit) is the major part of Smart Battery Power Management Unit (PMU) project. The Programming of Smart Battery PMU project is mainly divided into three parts which are: Serial Communication, graphical user interface (GUI) and the main classes.

5.1. Flowchart of Programming of PMU

At the beginning, the GUI is initialized. After that, universal serial bus (USB) to Serial Communication is initialized via getting port identifiers and searching a serial communication (COM) port element. If port enumeration contains more elements it returns the next element of this enumeration. If COM port is not found; the software returns error result. On the other hand, if COM port is found; then serial port and USB to Serial input/output (I/O) streams are opened, the event listeners are added, and the function checks while the input data is stated as sent and available. When the USB to Serial Communication is completed, the voltages are acquired. The acquired voltages are read. After reading voltages, the State of Charge (SoC) calculation function is called. Thereafter, the measurements are updated in GUI. When the measurements are updated then the program returns to get more voltage measurements.

Simultaneously, when the measurements are updated in GUI, the software gives users two choices which are shutting down the software or writing data to Microsoft Excel Sheet. The data is written to Microsoft Excel Sheet via creating a new excel file and sheet, instantiating cell objects and adding for the Excel sheet, writing cell voltages, SoC results, measurement counter and timestamp to file from measurement registers. When the data is written to Microsoft Excel sheet then the program returns to get more

voltage measurements. The full simplified and visualized flowchart is illustrated in Figure 22. The steps that the software follows are shown in the flowchart.

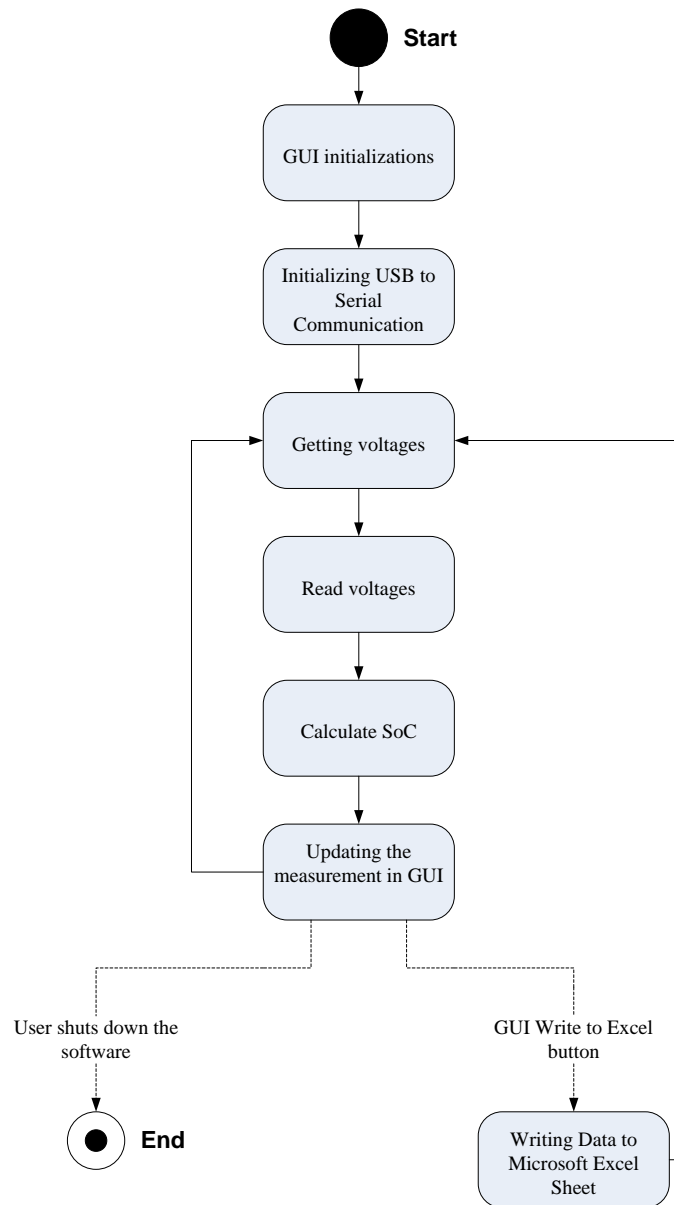


Figure 22. The flowchart of programming of PMU

5.2. Java Libraries

The core Java libraries are used for developing Smart Battery PMU which are listed in Table 18.

Table 18. The used core Java libraries

The core Java libraries			
java.awt	java.io	java.nio	java.text
java.util	javafx	javax.swing	jxl

The “java.awt” is utilized for generating user interfaces and graphics. Moreover, “java.io” is made use of providing system input and output via data streams and serialization. “java.nio” is used for defining buffers that are containers of data. “java.text” is used for processing texts and numbers. “java.util” is utilized for handling events, date and time. In addition, “javafx” is made use of ensuring the modern-looking user interface. “javax.swing” is used on top of the “java.awt”. Furthermore, “jxl” is utilized for writing, reading and updating Microsoft Excel sheets dynamically.

5.3. State of Charge (SoC) Calculation Function

The each battery cell voltage and SoC is set to 0 in code at the beginning of measurement.

The measurements are being updated by first, and individual Battery Management System (BMS) cell voltages are acquired and added together. Following this addition, the total voltages are divided to 24. As a consequence, total battery voltage is calculated. After that, SoC calculation method is called and those BMS cell voltages are placed to that method. Consequently, SoC of each cell is calculated. Then, all individual cell SoCs are added and divided to 24 to find total battery SoC.

6. RESULTS AND DISCUSSION

For testing the Power Management Unit (PMU), the software titled RFIC PMU GUI is used. A new graphical user interface (GUI) is designed for because it allows to record to excel, displays State of Charges (SoCs) and it is easy to use.

6.1. Graphical User Interface

The main GUI window given in Figure 23 displays the voltage and SoC status of 24 cells of the lead-acid battery pack. The total battery voltage is calculated by adding all series individual cell voltages. “Write to Excel” button is included to write measurement data to excel sheet. The PMU GUI is updated instantaneously. The data update rate including the delay is set by microcontroller.

For each cell there is a status indicator. If that status indicator shows “OK” it means the cell is in a safe condition. If that status indicator shows “OV” then the cell is overcharged (the cell voltage is higher than 2.15V). On the other hand, if that status indicator shows “UV” then the cell is undercharged (the cell voltage is less than 1.7V). Both the over & under voltage values are set in Java code and cannot be changed in GUI.

Differently from displaying each cell, the GUI also shows the total lead-acid battery pack voltage and SoC. It also plots total lead-acid battery SoC and voltage versus time.

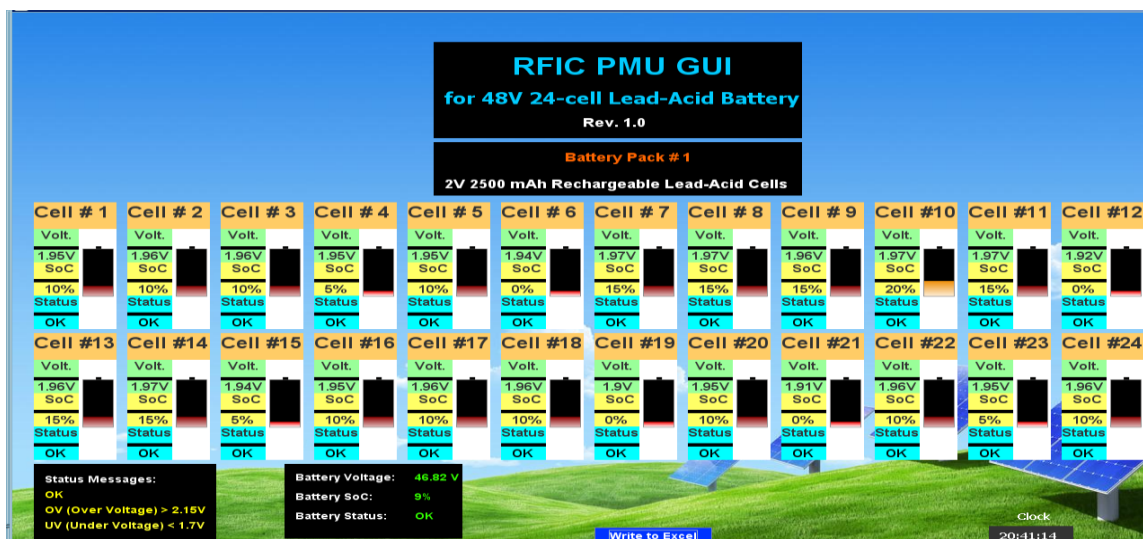


Figure 23. PMU GUI without charts

With this PMU GUI, the users can be aware of what is going on the lead-acid battery pack. The plots make it easier to obtain the variations by the time of progress. If the battery or cell status indicator is changed then the hardware should be fixed before any serious damage is caused. This PMU GUI allows the lead-acid battery for long-life operation by monitoring the voltages and SoCs of 24 lead-acid battery cells in a smart way. Only monitoring the voltages and SoCs is not enough for long-life operation. However, if the voltages and SoCs are not monitored then they could not be controlled.

The program immediately starts when it is run by the user. The only user-dependent function of program is “Write to Excel” function.

6.2. Cell Measurement Results

The Figure 24 shows the individual cell voltages and SoCs together with status indicator when the load is not connected at a given time.

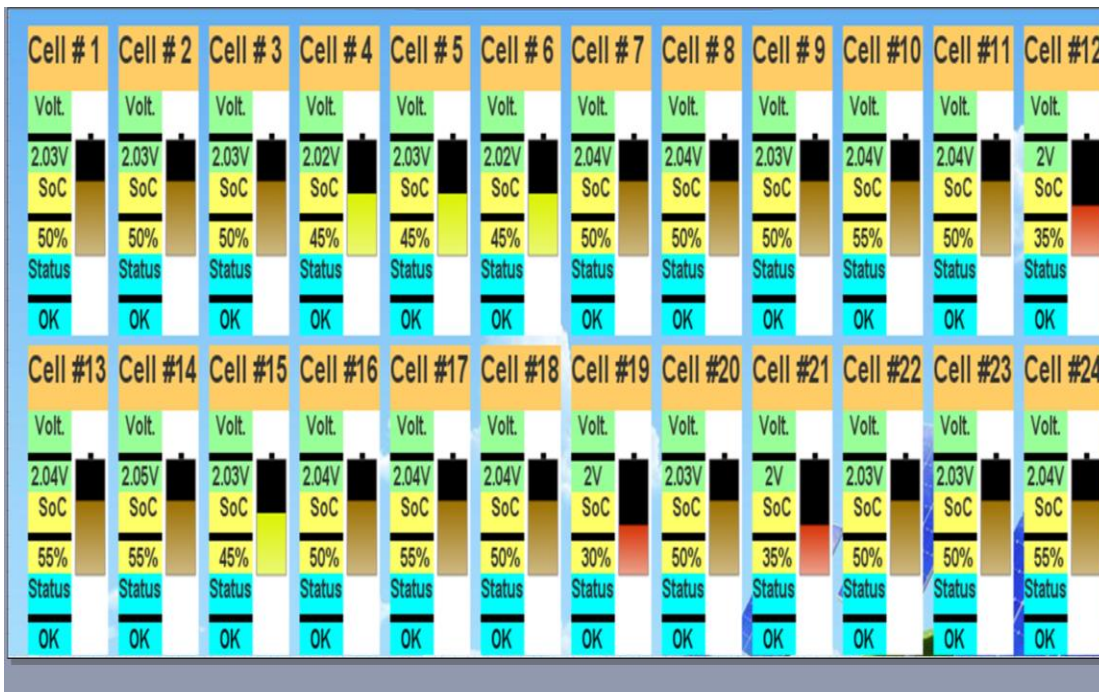












Figure 24. Individual cell voltages and SoCs

From the Figure 24, we can detect that Cell #19’s voltage status is less than other cells. The status indicator shows “OK”. However, it is going to enter a critical level (1.9V) in a time of period if it is not charged. In addition, Cell #12 and Cell #21’s SoC status’ are less than 40% and they should also be handled well. According to the Figure 24, since not all cells are in a same voltage level, the passive or active balancing might be applied to obtain the optimal performance of lead-acid battery pack.

Furthermore, all lead-acid cells are in a safe voltage range because none of them is overcharged or undercharged.

The SoC icons are defined in GUI as given in Table 19. The intervals are defined based on Table 5.

Table 19. SoC (%) and SoC Icon with respect to it

SoC (%)	SoC Icon
[90-100]	
[80-90)	
[70-80)	
[60-70)	
[50-60)	
[40-50)	
[30-40)	
[20-30)	
[10-20)	
[0-10)	

6.2.1. GUI Chart Results

The measurement result at a certain time is removed from the charts after one hour. In other words, measurement results last for one hour in GUI charts and new measurement results are shown. The measurement results shown in Chapter 6.2.1 are taken without using load. In Figure 25, variation of total 24-cells battery SoC in 15 seconds is given.

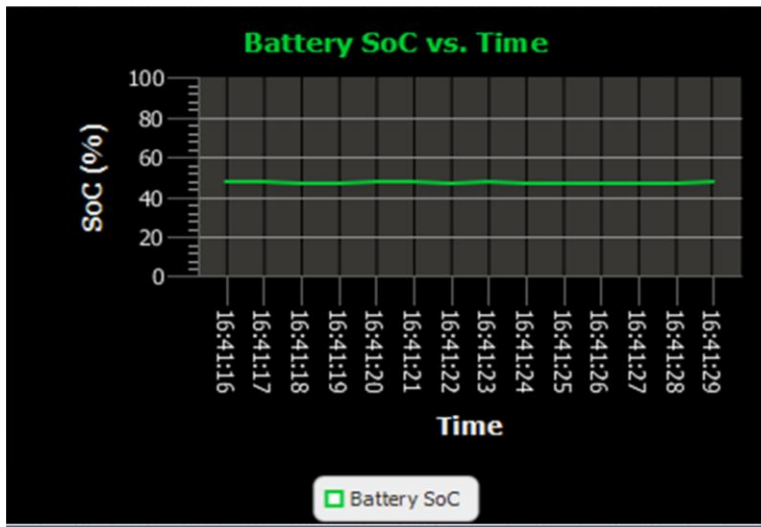


Figure 25. Total Battery SoC vs. Time

The small fluctuations can be seen in 15 seconds from Figure 25.

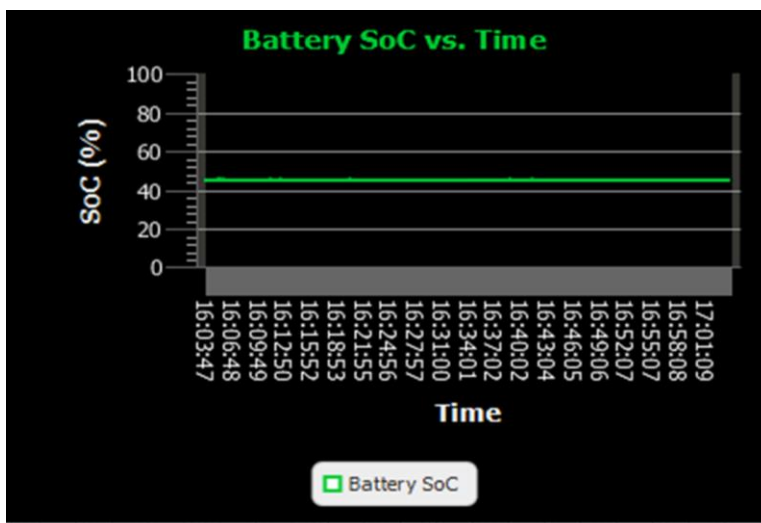


Figure 26. Total Battery SoC vs. Time in a different period of time

The whole 24-cells battery SoC remains almost in a same level, 48%, in one hour. However, in some periods the variations can be observed from Figure 26.

In the Figure 27, the variation of total 24-cells battery voltage in 15 seconds is given.

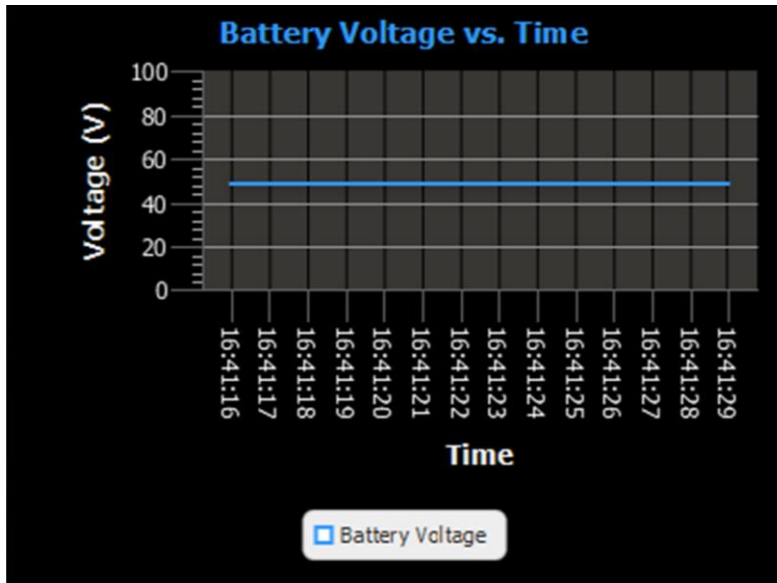


Figure 27. Total Battery Voltage vs. Time

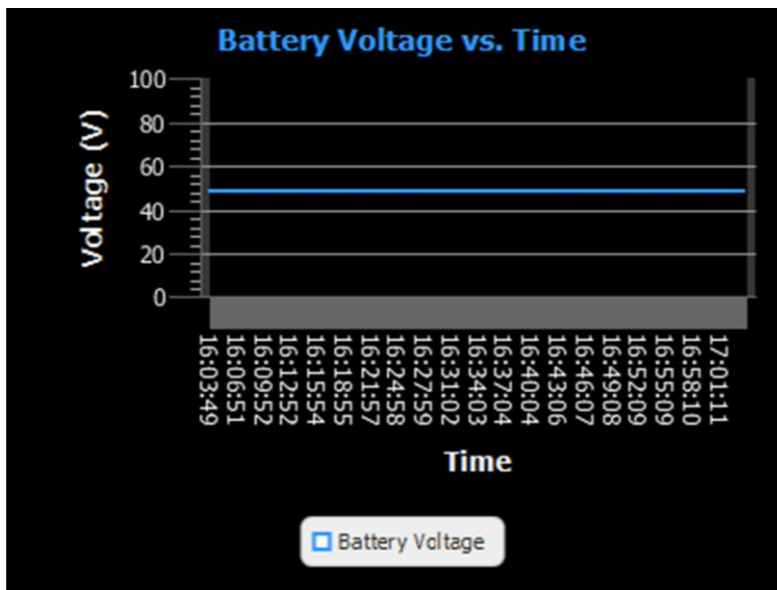


Figure 28. Total Battery Voltage vs. Time in a different period of time

From Figure 28, the total 24-cells battery voltage is approximately equal to 48V. As it is discussed in section 2.4, a SoC calculation algorithm is applied to estimate SoC of battery cell voltages. In a few words, it is estimation. However, the total battery voltage is directly shown in GUI charts without any estimation or calculation. Therefore, it is also obtained from Figures 27 and 28 that the total battery voltage is more stable than total battery SoC.

In the Figure 29, the instantaneous total battery voltage, SoC and status are given.



Figure 29. Instantaneous Battery Voltage, SoC and Status

According to the Figure 29, it can be acquired the battery is in a safe condition because the total battery SoC is more than 40%. The total battery is charged 48% and its voltage is 48.74V. The clock is also added to GUI so the users can observe battery voltage, SoC and status at any time.

6.2.2. Excel Results

The Excel sheet displays the measurement counter, cell voltages, cell SoCs, date and time. The measurement counter is updated every second.

Count	Cell1(V)	Cell2(V)	Cell3(V)	Cell4(V)	Cell5(V)	Cell6(V)	Cell7(V)	Cell8(V)	Cell9(V)	Cell10(V)	Cell11(V)	Cell12(V)	Cell13(V)	Cell14(V)	Cell15(V)
1	2,11	2,12	2,12	2,11	2,11	2,11	2,14	2,13	2,13	2,14	2,13	2,10	2,12	2,13	2,11
2	2,12	2,12	2,12	2,11	2,11	2,11	2,14	2,13	2,13	2,14	2,13	2,10	2,12	2,13	2,11
3	2,11	2,12	2,12	2,11	2,11	2,11	2,14	2,13	2,13	2,14	2,13	2,10	2,12	2,13	2,11
4	2,12	2,12	2,12	2,11	2,11	2,11	2,14	2,13	2,13	2,14	2,13	2,10	2,12	2,13	2,11
5	2,11	2,12	2,12	2,11	2,11	2,11	2,14	2,13	2,13	2,14	2,13	2,10	2,12	2,13	2,11
6	2,12	2,12	2,12	2,11	2,11	2,11	2,14	2,13	2,13	2,14	2,13	2,10	2,12	2,13	2,11
7	2,11	2,12	2,12	2,11	2,11	2,11	2,14	2,13	2,13	2,14	2,13	2,10	2,12	2,13	2,11
8	2,11	2,12	2,12	2,11	2,11	2,11	2,14	2,13	2,13	2,14	2,13	2,10	2,12	2,13	2,11
9	2,12	2,12	2,12	2,11	2,11	2,11	2,14	2,13	2,13	2,14	2,13	2,10	2,12	2,13	2,11
10	2,11	2,12	2,12	2,11	2,11	2,11	2,14	2,13	2,13	2,14	2,13	2,10	2,12	2,13	2,11
11	2,12	2,12	2,12	2,11	2,11	2,11	2,14	2,13	2,13	2,14	2,13	2,10	2,12	2,13	2,11
12	2,12	2,12	2,12	2,11	2,11	2,11	2,14	2,13	2,13	2,14	2,13	2,10	2,12	2,13	2,11
13	2,12	2,12	2,12	2,11	2,11	2,11	2,14	2,13	2,13	2,14	2,13	2,10	2,12	2,13	2,11
14	2,11	2,12	2,12	2,11	2,11	2,11	2,14	2,13	2,13	2,14	2,13	2,10	2,12	2,13	2,11

Figure 30. Cell voltages and measurement counter displayed in Excel sheet

From the Figure 30, the changes of each cell voltages with respect to the measurement counter can be obtained. The first label is measurement counter. After that, the results of voltages of 24 cells are located in labels.

The labels that show SoC results of 24 cells follow the labels that show the voltage results of 24 cells.

SoC12(%)	SoC13(%)	SoC14(%)	SoC15(%)	SoC16(%)	SoC17(%)	SoC18(%)	SoC19(%)	SoC20(%)	SoC21(%)	SoC22(%)	SoC23(%)	SoC24(%)	Date&Time
80,00	90,00	90,00	80,00	85,00	90,00	90,00	75,00	90,00	75,00	90,00	90,00	95,00	2013/12/17 18:25:51
80,00	90,00	90,00	80,00	90,00	90,00	85,00	75,00	90,00	75,00	90,00	90,00	95,00	2013/12/17 18:25:52
80,00	90,00	90,00	85,00	85,00	90,00	85,00	75,00	90,00	80,00	90,00	90,00	95,00	2013/12/17 18:25:53
80,00	90,00	90,00	80,00	85,00	90,00	90,00	75,00	90,00	75,00	90,00	90,00	95,00	2013/12/17 18:25:54
80,00	90,00	90,00	80,00	85,00	90,00	85,00	75,00	90,00	75,00	90,00	90,00	95,00	2013/12/17 18:25:55
80,00	90,00	90,00	80,00	85,00	90,00	85,00	75,00	90,00	75,00	90,00	90,00	95,00	2013/12/17 18:25:56
80,00	90,00	90,00	85,00	85,00	90,00	85,00	75,00	90,00	75,00	90,00	90,00	95,00	2013/12/17 18:25:57
80,00	90,00	90,00	85,00	85,00	90,00	85,00	75,00	90,00	75,00	90,00	90,00	95,00	2013/12/17 18:25:58
80,00	90,00	90,00	85,00	90,00	90,00	85,00	75,00	90,00	75,00	90,00	90,00	95,00	2013/12/17 18:25:59
80,00	90,00	90,00	80,00	85,00	90,00	90,00	75,00	90,00	80,00	90,00	90,00	95,00	2013/12/17 18:26:00
80,00	90,00	90,00	80,00	85,00	90,00	85,00	75,00	90,00	80,00	90,00	90,00	95,00	2013/12/17 18:26:01
80,00	90,00	90,00	85,00	85,00	90,00	85,00	70,00	90,00	75,00	90,00	90,00	95,00	2013/12/17 18:26:02
80,00	90,00	90,00	85,00	85,00	90,00	90,00	75,00	90,00	80,00	90,00	90,00	95,00	2013/12/17 18:26:03
80,00	90,00	90,00	80,00	85,00	90,00	85,00	75,00	90,00	75,00	90,00	90,00	95,00	2013/12/17 18:26:04

Figure 31. Cell SoC and date & time displayed in Excel sheet

From the Figure 31, the changes of each cell SoC with respect to the date & time can be obtained.

6.3. Load Discharging Curve

The load discharging curves help to observe the health of battery cells. The battery cell discharge performance depends on the load and how they are used. In Figure 32, the behavior of total battery voltage with respect to time when the load is connected is illustrated.

The current through the load is 0.74A at the beginning of discharging process. It is dropped to 0.72A at the end of the discharging process. Therefore, there is a 0.02A difference between the beginning and end of discharging process.

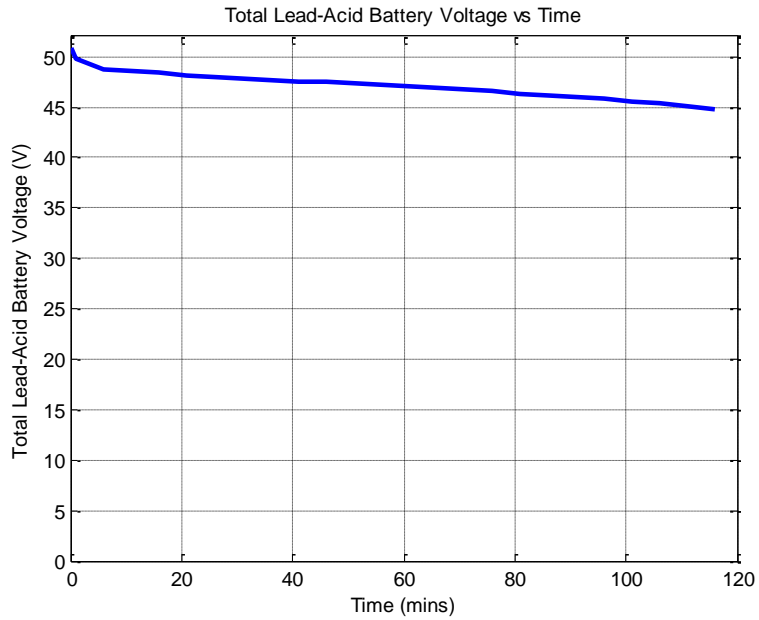


Figure 32. Total lead-acid battery voltage versus time

In the Figure 32, the total battery voltage is 50.87V at the beginning. After 116 minutes it is dropped to 44.8V.

Apart from Figure 32, in Figure 33 when the load is connected the load discharging curve of lead-acid battery cell #19 with respect to time is given.

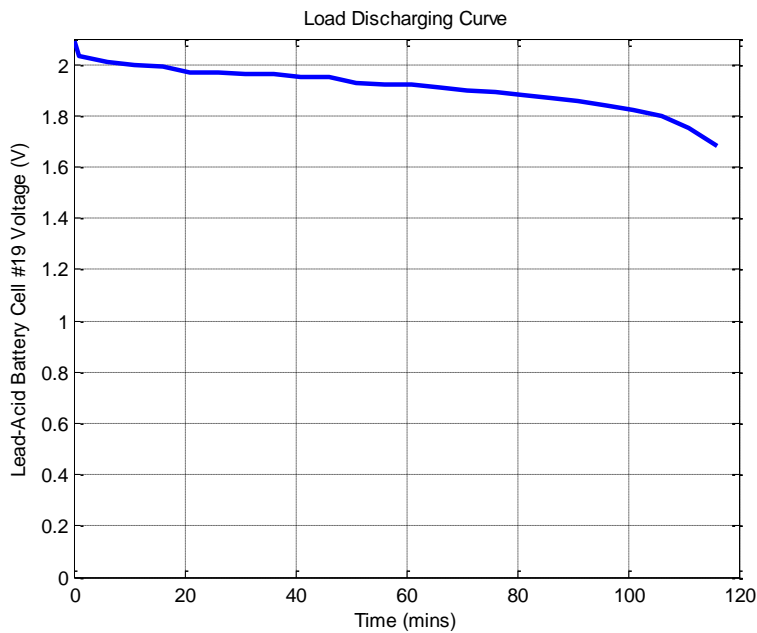


Figure 33. Load Discharging Curve of lead-acid battery cell #19

From Figure 33, it is obtained the power delivered by cells with the inclined discharge curve drops during the discharge cycle. The lead-acid battery cell #19 voltage is 2.09V at the beginning. After 116 minutes it is fallen to 1.68V. The measurement is stopped when the least charged lead-acid battery cell (cell #19) is less than 1.7V. Here, 1.7V is the critical level that states the lead-acid battery cell is fully discharged (Enersys Cyclon 2008).

In addition, since the constant current load is used for the discharging process, the 0.02A variation between the beginning and end is acceptable.

Furthermore, the lead-acid battery cells must be fully charged after every discharging process and they need to be kept charged at a floating voltage which is more than the nominal voltage.

After the discharging process and load is disconnected from the setup, the battery cell voltages are also measured by the MS8221D multimeter (Mastech 2013). The comparison between the GUI and multimeter measurements are given in Table 20.

Table 20. Comparison of GUI and multimeter lead-acid battery cell measurements

	GUI	Multimeter
Cell #1	1.95	1.94
Cell #2	1.96	1.95
Cell #3	1.96	1.95
Cell #4	1.95	1.94
Cell #5	1.95	1.94
Cell #6	1.94	1.93
Cell #7	1.97	1.96
Cell #8	1.97	1.96
Cell #9	1.96	1.96
Cell #10	1.97	1.97
Cell #11	1.97	1.96
Cell #12	1.92	1.91
Cell #13	1.96	1.96
Cell #14	1.97	1.96
Cell #15	1.94	1.93
Cell #16	1.95	1.95
Cell #17	1.96	1.95
Cell #18	1.96	1.95
Cell #19	1.9	1.89
Cell #20	1.95	1.95
Cell #21	1.91	1.91
Cell #22	1.96	1.95
Cell #23	1.95	1.94
Cell #24	1.96	1.96

From Table 20, it can be concluded that the GUI shows correct results. The 0.5% difference between the GUI and multimeter measurements is acceptable. The difference might be caused by rounding, tolerances and/or cable losses.

7. CONCLUSIONS

In conclusion, this MSc. Thesis studies the smart battery PMU for a 48V battery pack of series-connected 24 lead-acid cells. An alternative voltage and SoC monitoring system is proposed for current Battery Management Systems which monitors the voltages and SoCs of lead-acid battery cells properly during both charging and discharging. In addition, the software allows users to save measurement data to utilize them whenever it is required. The main goal which is set before the MSc. Thesis is achieved.

During the MSc. Thesis project; at first the initial calculations are performed, after that initial calculation results are applied in system prototype with minor modifications. Later on, system is designed with the Java software to control whole PMU system.

The proposed system for the smart battery PMU monitors the individual lead-acid cell's performance using the microcontroller board Arduino Due. The Arduino Due communicates with MAX11068 EVKit through an I²C bus. The Arduino Due provides communication for measurements of the voltages of each cell and based on those cell voltage measurements the SoCs are calculated by the Java program. The Arduino Due commands are written based on Maxim Integrated (2010).

Although this smart battery PMU is designed on a battery back of 24 lead-acid cells, the complete system can be used for a lead-acid battery pack of any size (up to 372 cells) with minor modifications in the system. The software allows users to make minor modifications for possible future requirements.

It is proved that the software is measuring lead-acid cell voltages accurately (with an error margin of 0.5%). The 0.5% difference between the GUI and multimeter measurements is admissible.

To improve this Smart Battery PMU project, the possible future design is discussed.

As a consequence, this MSc. Thesis is a part of major KERS project (Tampere University of Technology RF Integrated Circuits Laboratory 2013) that is going to interact with the DC/DC converter and motor controller for mobile or stationary high volume applications. The KERS project requires a 48V battery which provides energy to DC/DC converter and motor controller. Also, the DC/DC converter and motor controller restore energy to 48V battery. Hence, this MSc. Thesis can be used for the bigger KERS project as it is a 48V smart battery PMU which allows providing and restoring energy, and provides an accurate voltage and SoC monitoring system.

8. CONTINUATION DESIGN OF WORK

The whole system is done by RFIC Laboratory Research Group. The future BMS/PMU block diagram plan is designed and illustrated in Figure 34. It will be mainly consisted of source, control and load parts. In this MSc. Work, I work in the monitoring part of the system. In Figure 34, the communications between 48V 24-cell lead-acid battery, microcontroller (Arduino) and MAX11068 EVKits in control part are already done. My MSc. work can be improved by the block diagram given in Figure 34.

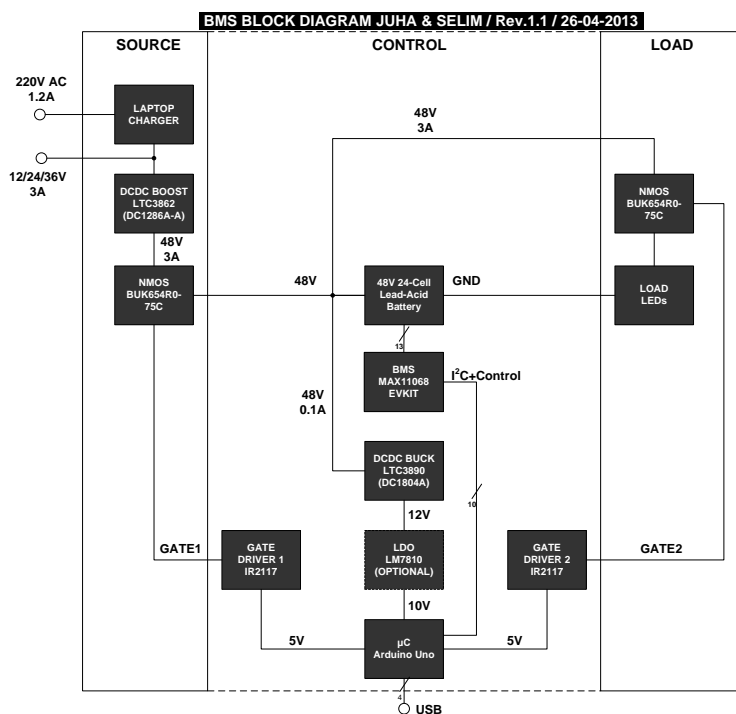


Figure 34. Future BMS/PMU Block Diagram

The source part is consisted of charger, step-up DC/DC converter and metal-oxide-semiconductor (MOS) switch. The charger is selected so that the output of charger should be 12V, 24V or 36V. LTC3862 is placed at the output of charger, which is a step-up DC/DC converter (Linear Technology 2008). The output of LTC3862 is 48V with a current of 3A. Two BUK654R0-75Cs are used as MOS switches.

The control part is consisted of gate drivers, 24-cell lead-acid batteries, MAX11068 evaluation kit (EVKit) (as a BMS), Arduino Uno (as a microcontroller), and an optional

low-dropout regulator (LDO). In addition, Arduino Due can be replaced with Arduino Uno. The major difference for this design is that Arduino Due's operating voltage is 3.3V. Two IR2117s are planned to use as high side gate drivers and for level shifting purpose. However, there are some limitations to use them. IR2117s have a bootstrap capacitor that pulls the logic supply voltage into gate node when it turns on. The supply voltage charge in capacitor lasts for only couple milliseconds. Next, another pulse is needed for input pin. Hence, IR2117s can be only used with a 1+ kHz pulse width modulation (PWM) signal. Thus, two IR2117s can be replaced in future. High side gate driver configuration needs a switch between the load and supply. The MOS gate is pulled high to turn on the high side gate driver. With the usage of them, the Arduino Uno can control the switches both on source and load sides. Otherwise, the Arduino Uno cannot control the switches as its operating voltage is 5V. Furthermore, the Arduino Uno requires input voltage between 7V to 12V to operate. This operating voltage is gained through a DC/DC step-down process. For this purpose, LTC3890 DC/DC step-down converter is added to design. LTC3890 takes the 48V input voltage and gives 12V output voltage (Linear Technology 2010). Additionally, the MAX11068 EVKit is used as BMS. The inter-integrated circuit (I²C) communication and control of MAX11068 is provided by the microcontroller. The LDO is optional but it provides filtering and drops out the output voltage of LTC3890. LM7810 can be used as a LDO in this design to drop 12V out to 10V (Fairchild Semiconductor 2013).

The load part is consisted of MOS switch and the light-emitting diodes (LEDs) which are used as a load. The load is connected to MOS switch and the output of 24-cell lead-acid battery.

Nevertheless, the future BMS/PMU can display temperature and current measurements of each battery cells. In addition, the portability of the system could be increased with researching wireless capabilities. The experiments are done with 24 lead-acid battery cells. However, considering the MAX11068 specifications in future the system can be designed to be scalable up to 372 cells.

Nonetheless, an alarming function could be added to the BMS/PMU. The complete BMS/PMU can make use of the alarming function if any system parameters exceed their operating levels. Also, if the number of series connected battery cells create a high voltage level for applications then the cell balancing should be implemented in future design to prevent the potential damage. The active balancing method can be applied for this purpose because the active balancing method is faster and the power efficiency of it is higher than the passive balancing method.

Consequently, the control of the PMU can be mainly divided into four parts: Avoidance of over/undercharging of battery cells, monitoring battery temperature, monitoring battery output current, and controlling the switching process.

REFERENCES

Andrea, D. 2010. “Battery Management Systems for Large Lithium-Ion Battery Packs”. Artech House.

Arduino. “Arduino Due”. [Accessed on 18.04.2013]. Available at:
<http://arduino.cc/en/Main/arduinoBoardDue>

Arduino. “SAM3X-Arduino Pin Mapping”. [Accessed on 18.04.2013]. Available at:
<http://arduino.cc/en/Hacking/PinMappingSAM3X>

Arduino. “Arduino Uno”. [Accessed on 18.04.2013]. Available at:
<http://arduino.cc/en/Main/arduinoBoardUno>

Arduino. “Wire Library”. [Accessed on 18.04.2013]. Available at:
<http://arduino.cc/en/reference/wire>

Arendarik, S. 2012. “Active Cell Balancing in Battery Packs”. Freescale Semiconductor, Inc. [Accessed on 18.04.2013]. Available at:
http://www.freescale.com/files/32bit/doc/app_note/AN4428.pdf

Atmel. “SAM3X/A”. [Accessed on 18.04.2013]. Available at:
<http://www.atmel.com/Images/doc11057.pdf>

Begovic M. 2012. “Electrical Transmission Systems and Smart Grids”. Springer.

Bergveld, H.J. Kruijt, W.S. Notten, P.H.L. 2002. “Battery Management Systems – Design by Modelling”. Kluwer Academic Publishers. Boston.

Broussely, M. Pistoia, G. 2007. “Industrial Applications of Batteries”. First Edition. Elsevier B.V. Amsterdam, The Netherlands.

Clarke, R.S. 2011. "B-LAB: CHANGING THE GAME FOR LEAD ACID". Applied Intellectual Capital. Alameda. [Accessed on 24.09.2013]. Available at: http://www.battcon.com/PapersFinal2011/ClarkeStephenPaperDONE2011_13.pdf#!.

Claus, D. 2008. "Materials and processing for lithium-ion batteries". Volume 60, Issue 9, pp 43–48.

Energys Cyclon. 2008. "US-CYC-ApplicationManual-007_04081".

Fairchild Semiconductor. 2013. "LM78XX / LM78XXA 3-Terminal 1 A Positive Voltage Regulator". [Accessed on 19.04.2013]. Available at: <http://www.fairchildsemi.com/ds/LM/LM7805.pdf>

Huet, F.1998. "A review of impedance measurements for determination of the state-of-charge or state-of-health of secondary batteries". Elsevier Science S.A.

Hyperion. "HYPERION AC/DC EOS0606iAD-C USER'S MANUAL". [Accessed on 23.04.2013]. Available at: [http://media.hyperion.hk/dn/EOS/EOS0606iAD\(acdc\)-A-MAN-EN.pdf](http://media.hyperion.hk/dn/EOS/EOS0606iAD(acdc)-A-MAN-EN.pdf)

International Rectifier. 2007. "IR2117(S)/IR2118(S) & (PbF)". [Accessed on 20.04.2013]. Available at: <http://www.irf.com/product-info/datasheets/data/ir2117.pdf>

Kong-Soon, N. Chin-Sien, M. Yi-Ping, C. Yao-Ching, H. 2008. "State-of-Charge Estimation for Lead-Acid Batteries Based on Dynamic Open-Circuit Voltage". 2nd IEEE International Conference on Power and Energy (PECon 08). Johor Baharu, Malaysia.

Krein, P. T. Balog, R. 2002. "Life Extension Through Charge Equalization of Lead-Acid Batteries". [Accessed on 18.04.2013]. Available at: <http://windandsunpower.com/Download/intelec02.pdf>

Linden, D. Reddy, T. B. 2002. "HANDBOOK OF BATTERIES". Third Edition. McGraw-Hill. New York.

Linear Technology. 2008. "LTC3862 Multi-Phase Current Mode Step-Up DC/DC Controller". [Accessed on 20.04.2013]. Available at: <http://cds.linear.com/docs/en/datasheet/3862fb.pdf>

Linear Technology. 2010. "LTC3890 60V Low I_Q, Dual, 2-Phase Synchronous Step-Down DC/DC Controller". [Accessed on 19.04.2013]. Available at:

<http://cds.linear.com/docs/en/datasheet/3890fc.pdf>

Linear Technology. 2013. "LTC6804-1/LTC6804-2 Multicell Battery Monitors".

Mastech. 2013. "MS8221D DIGITAL MULTIMETER". [Accessed on 17.12.2013].

Available at: <http://www.p-mastech.com/images/SPEC/ms8221d%20ms8230b.pdf>

Maxim Integrated. 2008. "Maxim MINIUSB User Guide". [Accessed on 04.04.2013].

Available at: <http://datasheets.maximintegrated.com/en/ds/MINIUSB.pdf>

Maxim Integrated. 2010. "MAX11068 12-Channel, High-Voltage Battery Sensor, Smart Data-Acquisition Interface".

Maxim Integrated. 2012. "Automotive Product Guide". [Accessed on 04.10.2013].

Available at:

<http://digichip.ru/datasheet/PDF/708f64cd8fd71531242118389f171796/6cc98ba2045fe4098d24356d14447085/MAX2135AETNV+.pdf>. p. 29.

Maxim Integrated. 2013. "Evaluation System for the MAX11068". [Accessed on 04.04.2013]. Available at:

<http://www.maximintegrated.com/datasheet/index.mvp/id/6882>.

Maxim Integrated. 2013. "MAX17830 12-Channel, High-Voltage Battery Sensor with Advanced SMBus Ladder and External Cell Balancing". [Accessed on 04.10.2013].

Available at: <http://www.maximintegrated.com/datasheet/index.mvp/id/7114>.

Miller, P. 2012. "xEV market trend and prospect". 2012 IEEE Vehicle Power and Propulsion Conference. Seoul, Korea.

National Geographic 2004. "The End of Cheap Oil". vol. 205, no. 6.

NetBeans. 2013. "Welcome to the NetBeans Community". [Accessed on 09.05.2013].

Available at: <https://netbeans.org/about/index.html>

NXP Semiconductors. "UM10204, I2C-bus specification and user manual". Rev. 5-9 October 2012.

Pang, S. Farrell, J. Du, J. Barth, M. 2001. "Battery State-of-Charge Estimation". Proceedings of the American Control Conference, vol. 2.

Pistoia, G. 2005. "Batteries for Portable Devices". Elsevier B.V. Amsterdam, The Netherlands.

Pistoia, G. 2009. "Battery Operated Devices and Systems". First Edition. Elsevier B.V. Amsterdam, The Netherlands.

Racherla, K. 2011. "Measure Multiple Temperatures in Battery-Management Systems, and Save Power Too". [Accessed on 07.10.2013]. Available at:
http://www.eetasia.com/STATIC/PDF/201205/EEOL_2012MAY03_POW_TEST_AN_01.pdf?SOURCES=DOWNLOAD

Rahimi-Eichi, H., Ojha, U., Baronti, F., Chow, M. 2013. "Battery Management System: An Overview of Its Application in the Smart Grid and Electric Vehicles," Industrial Electronics Magazine, IEEE, vol.7, no.2.

Reddy, T. B. 2011. "Linden's Handbook of Batteries". Fourth Edition. McGraw-Hill. New York.

Tampere University of Technology RF Integrated Circuits Laboratory. 2013. "Mobile / Stationary Big Volume Applications". [Accessed on 09.01.2014]. Available at:
<http://www.cs.tut.fi/tlt/rfasic/RFCCLab.pdf>

Tanaami, A. Morimoto, M. 2009. "On-line Estimation of SOH for Lead-Acid Battery". PEDS 2009. International Conference on Power Electronics and Drive Systems. Taipei, Taiwan, R.O.C.

Texas Instruments. 2006. "bq20z80 Application Book".

Texas Instruments. 2012. "Wide Range Fuel Gauge with Impedance Track™ for Lead-Acid Batteries" [Accessed on 04.10.2013]. Available at:
<http://www.ti.com/lit/ds/slusb55a/slusb55a.pdf>

The Boston Consulting Group Inc. 2010. "Batteries for Electric Cars; Challenges, Opportunities, and the Outlook to 2020". Boston, MA, USA. [Accessed on 19.04.2013]. Available at: <http://www.bcg.com/documents/file36615.pdf>

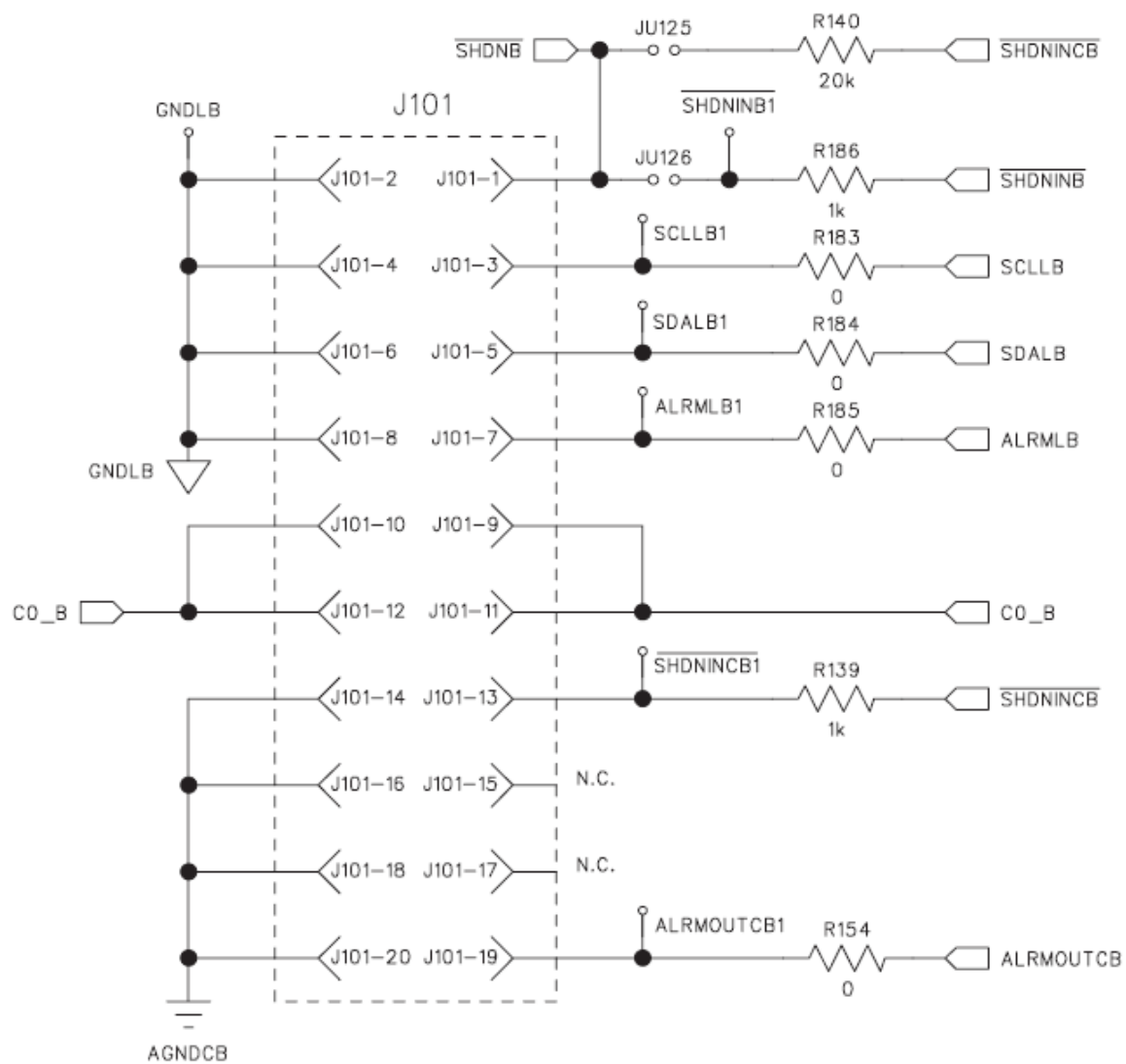
Wang, P., Liang, B., Ye, X., Ko, W.H., Cong P. 2010. "A Simple Novel Wireless Integrated Power Management Unit (PMU) for Rechargeable Battery-Operated Implantable Biomedical Telemetry Systems," Bioinformatics and Biomedical Engineering (iCBBE), 4th International Conference. Chengdu.

Wikipedia. 2009. "Grid storage energy flow". [Accessed on 12.04.2013]. Available at: http://en.wikipedia.org/wiki/File:Grid_storage_energy_flow.png.

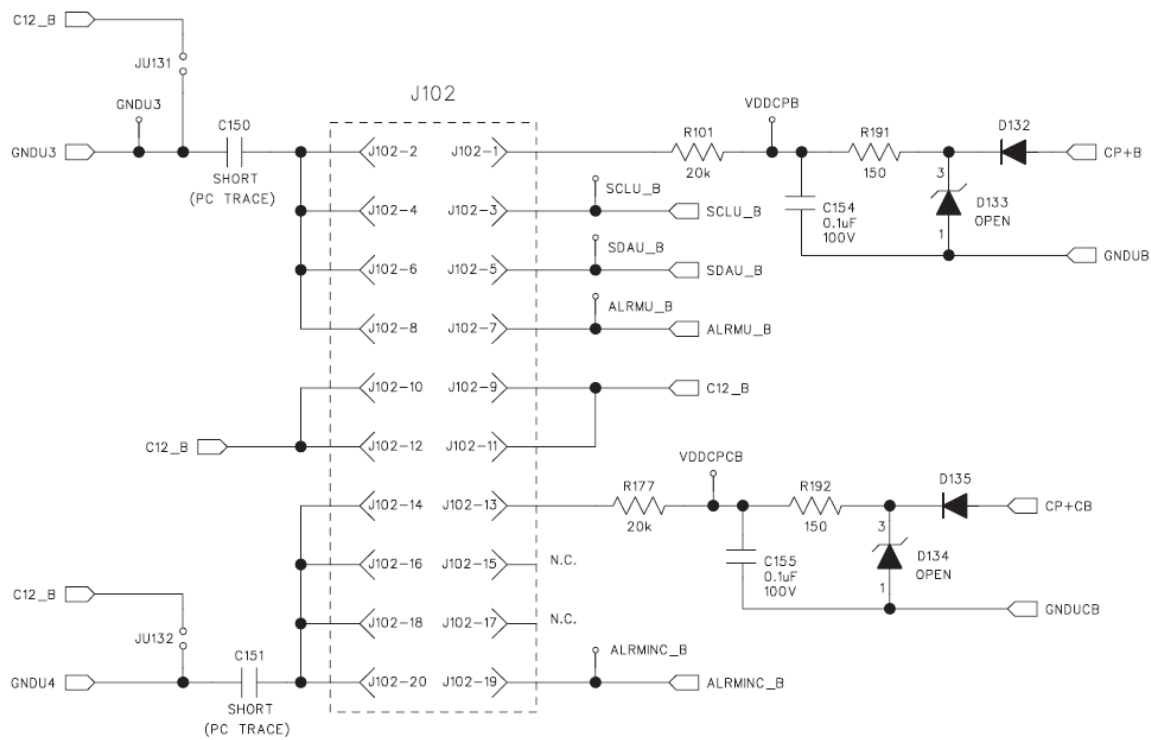
Williams, D. 2012. "Configuring the bq34100 Data Flash". Texas Instruments.

APPENDIX 1: MAX11068 EVKIT CELL CONFIGURATION HEADERS AND SWITCH

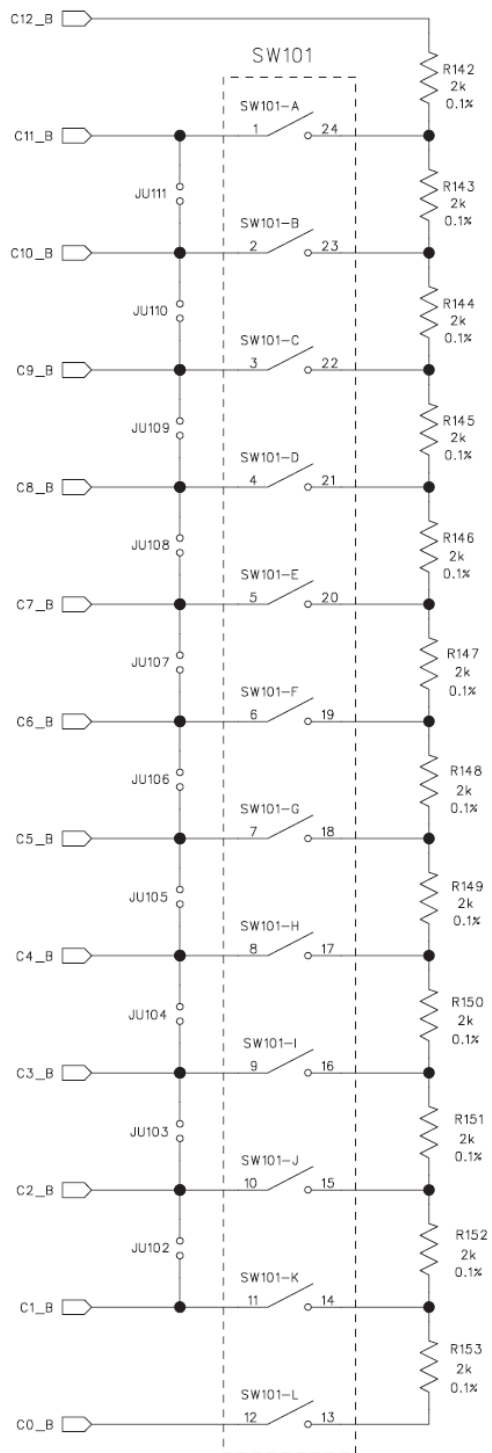
MAX11068 EVKit's cell configuration header J101 is given below (Maxim Integrated 2013).



MAX11068 EVKit's cell configuration header J102 is given below (Maxim Integrated 2013).

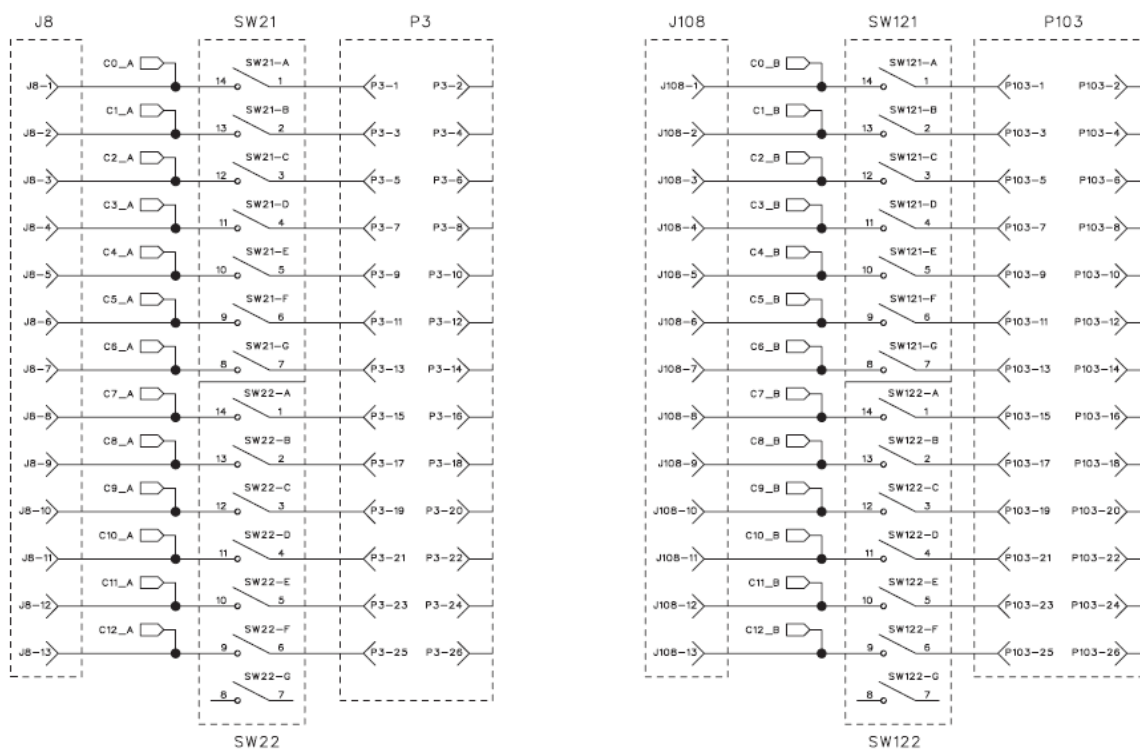


MAX11068 EVKit's cell configuration switch SW101 is given below (Maxim Integrated 2013).



APPENDIX 2: MAX11068 EVKIT CELL CONNECTION SWITCHES AND HEADERS

MAX11068 EVKit's cell connection switches and headers are given below (Maxim Integrated 2013).



APPENDIX 3: DISCHARGING ENERSYS CYCLON BATTERIES

In the table below, the recommended EODV with respect to the Discharge Rate is given (Enersys Cyclon 2008).

Discharge Rate (A)	Minimum EODV/cell (V)
0.05C ₁₀	1.75
0.1C ₁₀	1.7
0.2C ₁₀	1.67
0.4C ₁₀	1.65
C ₁₀	1.6
2C ₁₀	1.55
4C ₁₀	1.5

APPENDIX 4: TIMING OF PARAMETER UPDATES DURING THE RELAXATION MODE FOR STATE OF HEALTH ESTIMATION

During the relaxation mode, the timing of DoD_0 and Q_{max} updates are given below (Texas Instruments 2006).

